NATIONAL ADVISORY COMMITTEE FOR AERONAUTICS

TECHNICAL NOTE 2254

REGENERATOR-DESIGN STUDY AND ITS APPLICATION TO TURBINE-PROPELLER ENGINES

By S. V. Manson

Lewis Flight Propulsion Laboratory
Cleveland, Ohio

Washington
January 1951

NATIONAL ADVISORY COMMITTEE FOR AERONAUTICS

TECHNICAL NOTE 2254

REGENERATOR-DESIGN STUDY AND ITS APPLICATION TO TURBINE-PROPELLER ENGINES

By S. V. Manson

SUMMARY

A comprehensive study is presented of regeneration as a means of improving the load-range performance of turbine-propeller aircraft. The efficacy of regeneration for turbine-propeller engines was evaluated by comparing the cargo capacity of a typical airplane powered by a regenerated engine with the cargo capacity of an airplane powered by an unregenerated engine. In each case, the turbine-propeller engine had a compressor of optimum pressure ratio for the operating conditions investigated and the regenerated engine had the optimum regenerator core among the many designed for the study.

Conditions at which the comparisons were made included: combustion temperatures of 1600° and 2500° F; regenerator warming effectivenesses from 0 to 0.9; altitudes of 0 and 30,000 feet; flight speeds of 218, 300, and 400 miles per hour; and flight distances up to 9000 miles.

Results indicated that gains from regeneration are small except near sea level for flight distances of 3000 or more miles and at speeds of about 300 miles per hour. The largest gains computed in this analysis are given in the following table:

Altitude (ft)	Combustion temperature (°F)	Regenerator warming effectiveness	Flight speed (mph)	Flight distance (miles)	Increase in cargo capacity due to regeneration (lb/thp)	Increase in cargo capacity due to regeneration (lb/ton airplane gross weight)
0	1600	0.50	218	3000	0.51	36
			218	5000	.90	64
			300	3000	.38	56
			400	1000	-.10	-32
30,000	1600	0.50	218	6000	0.35	26
			300	6000	.32	28
			400	3000	-.05	-7
	2500	0.50	218	9000	0.49	38
			300	8000	.38	34
			400	5000	.14	20

Inasmuch as duct weights and duct pressure drops were neglected in the analysis, actual regenerative gains would be somewhat smaller than those tabulated. The gains shown are only one-third to one-half of those that would result from regenerator cores of zero weight and zero fluid pressure drops.

INTRODUCTION

The use of a regenerator to exchange heat between the turbine exhaust gas and the relatively cool compressed air has been under consideration as a means of decreasing the fuel consumption of turbine-propeller engines. The value of regeneration, which is well established for stationary power plants, is yet to be proven for aircraft power plants because the regenerator weight and fluid pressure drops may offset the decrease in fuel-air ratio achieved by regeneration.

The effect of counterflow-tubular regenerator cores of various weights on the performance of turbine-propeller engines for a limited range of engine operating conditions is reported in reference 1, where it is stated that profitable reductions in fuel consumption can be obtained by means of regenerators. The results of reference 1, however, are inconclusive because the gains indicated are for the nonoptimum range of compressor pressure ratios from 2 to 6 at both sea level and 25,000 feet and because the principal results are based on the assumption that the regenerated and unregenerated engines would operate at the same compressor pressure ratio.

In order to determine the potentialities of regenerators for turbine-propeller engines, a comprehensive investigation was conducted at the NACA Lewis laboratory including the:

1. Determination of optimum compressor pressure ratios for both regenerated and unregenerated engines

2. Design of a large number of high-performance regenerators as based on a detailed study of the heat-exchange effectiveness, weight, and fluid pressure drops of various regenerator core structures

3. Determination of the cargo-carrying capacity of a typical aircraft equipped with regenerated and unregenerated engines

In the load-range calculations employed for determining the aircraft cargo capacity with and without a regenerator, flight is assumed to be at constant power and altitude, with assumed values of airplane aspect ratio and viscous-drag coefficient typical of the values

attained in current efficient high-speed cargo airplanes. The effect of engine and regenerator weights and of regenerator pressure drops on the aircraft load-range performance is taken into account in all cases.

In order to facilitate cargo-capacity determinations, coordinates are presented on which the engine weight and the specific fuel consumption (with or without regenerator) can be plotted and the cargo capacity thereby quickly obtained for various engine-operating and flight conditions and regenerator designs.

From the results of this investigation, the regenerated and unregenerated engines, operating at their respective optimum compressor pressure ratios, are compared on the basis of pounds of cargo that can be carried per installed engine horsepower for flights of various distances. In this comparison, the regenerated engine is equipped with the regenerator core that was optimum among the various types calculated in the analysis.

METHODS AND REGENERATOR-CORE CONFIGURATIONS

Regenerative-Cycle Analysis

Engine specific fuel consumption and work per pound of air are calculated from the thermodynamic cycle of the working fluid. The unregenerative cycle of the turbine-propeller engine is well known and is schematically shown in figure 1. Regeneration may be effected by introducing a heat exchanger (regenerator), as schematically shown in figure 2. By means of the regenerator, heat is exchanged between the turbine exhaust gas and the relatively cool compressed air; the thermodynamic cycle then changes to that shown in figure 3.

The following range of conditions was investigated in the computation of the engine thermodynamic cycle:

Altitude, ft	0 and 30,000
Flight speed, mph	218, 300, and 400
Compressor pressure ratio	up to 50
Combustion temperature, $^{\circ}F$	1600 and 2500
Propeller- to jet-thrust ratio	optimum (reference 2)

The following constant values were used for component efficiencies:

Dynamic pressure recovery factor	0.75
Adiabatic total-to-total pressure compressor efficiency	0.85

Adiabatic total-to-total pressure turbine efficiency	0.85
Propeller efficiency	0.85
Combustor efficiency	1.0
Exhaust-nozzle efficiency	1.0
Combustion-chamber pressure drop	0
Regenerator-ducting pressure drop	0

For the case of a combustion temperature of 2500° F, the turbine was assumed to be liquid-cooled and the power output of the turbine was diminished by an amount equal to the required heat-dissipation rate to the coolant flowing through the turbine blades. This heat-dissipation rate was taken as that required to maintain the maximum permissible turbine-blade temperature, as dictated by blade-stress considerations (reference 3). In these calculations, reasonable current turbine-design practice was assumed. The heat-transfer coefficient from the gases to the turbine blades, which relates the temperature difference between gas and blade to the heat-dissipation rate, was computed by the following formula:

$$\frac{h}{c_p G} Pr^{2/3} = 0.198\left(\frac{\psi G}{\mu}\right)^{-0.321}$$

All symbols used herein are defined in appendix A. The weight of a standard liquid-to-air radiator required to dissipate the heat to the atmospheric cooling air was added to the engine weight in the over-all weight estimates.

The thermodynamic properties of the working fluid were obtained from reference 4. Fuel-air ratios required for the specified combustion temperatures were obtained from reference 5.

Engine Weights and Air Flows

The load-range performance of an aircraft involves the engine weight per unit horsepower (referred to herein as "specific weight"); in the determination of specific weight, the weight of engine and propeller per unit engine frontal area, the air flow per unit engine frontal area, and the engine work per pound of air must be known. The engine work per pound of air was obtained from the cycle analysis. The weight of engine and propeller per unit engine frontal area, as a function principally of compressor pressure ratio and combustion temperature, was calculated by a method developed in an unpublished

analysis by the NACA Lewis laboratory. The predicted weights checked within 10 percent of the weights of all the existing compressor-turbine engines.

The air flow was assumed to be 3 pounds per second per square foot of engine frontal area at sea level. The air flow was then taken proportional to the ambient-air density, thus resulting in an air flow per square foot of engine frontal area of 1.3 pounds per second at an altitude of 30,000 feet.

For higher air flows per unit engine frontal area, the basic engine weight would remain fixed for a given frontal area, whereas the regenerator weight would increase in proportion to the air flow. Hence with increased air flow, the ratio of the regenerator-to-engine weight would increase so that the gains due to regeneration would decrease. The regenerator gains evaluated herein can thus be expected to be somewhat greater than would be attained with engines having higher air flows.

Load-Range Performance

A basis for comparison of regenerated and unregenerated engines is the respective cargo capacities per installed horsepower in flights under identical conditions. The cargo capacity per installed horsepower is given simply as the difference between the weight assignable to engine (including propeller) plus cargo per installed horsepower and the engine specific weight. The weight assignable to engine plus cargo per installed horsepower was determined from load-range performance calculations made for various flight speeds, altitudes, distances, and engine specific fuel consumptions. The calculations were based on the load-range equations presented in appendix B for a flight plan of constant horsepower and constant altitude. Assumptions for the load-range calculation are typical of current efficient cargo airplanes and included the following:

Structure weight/gross weight	0.4
Fuel-tank weight, percent of gross fuel load	10
Effective aspect ratio	10
Viscous-drag coefficient	0.025
Wing loading, lb/sq ft	70

The weights assignable to engine plus cargo were found from the load-range calculations to be very nearly linear with specific fuel consumption for the flight speeds, the altitudes, and the flight distances investigated for this analysis.

In the determination of cargo capacity for the regenerated engine, the engine specific weight included the weight of the regenerator; the effect of regeneration on the weight assignable to engine plus cargo was introduced through its effect on the engine specific fuel consumption, as given from the cycle and regenerator-performance calculations.

Regenerator-Core Configurations

In order to determine the actual gains in cargo capacity achieved by regeneration, the actual regenerator weights and fluid pressure drops must be known. The following types of regenerator core were investigated:

(a) Crossflow plate and interrupted fin
(b) Crossflow plate and uninterrupted fin
(c) Crossflow tubular
(d) Counterflow tubular

The cores were designed on a per-pound-of-air-per-second basis and the core performance so obtained was independent of the engine frontal area or air flow.

Crossflow-plate and interrupted-fin core. - The configuration of the regenerator with the crossflow-plate and interrupted-fin core and the details of the core are presented in figure 4. The regenerator is assumed to be annular in shape. The air from the compressor flows axially through unfinned smooth passages and traverses the regenerator length twice. The gases from the turbine flow radially outward, in straight-through flow. The gas passages have strip fins that are interrupted in the direction of the gas flow and staggered in successive rows.

In the design calculations, the core inside and outside diameters were kept constant at 32 inches and 44 inches, respectively (r and H of fig. 4(a) are 16 in. and 6 in., respectively) for convenient installation on an existing turbine-propeller engine. As subsequently shown, however, substantial changes in core diameter can be made in a manner that produces practically no effect on final performance. In the design calculation, plate spacings in the gas and air passages, b and a, fin transverse spacing s, fin length λ, wall thickness of the basic heat-transfer metal t_w, and, in some cases, fin thickness δ were varied. With fixed-plate spacings b and a, the total number of plates N was determined by the requirement of fitting the regenerator within the specified core diameter. For each set of

values for core parameters and preassigned regenerator effectivenesses, the length L and the resultant pressure drops were computed. Ranges of core parameters investigated for these regenerators, as well as for the other regenerator-core types, are presented in table I.

Crossflow-plate and uninterrupted-fin core. - The assumed configuration of the regenerator with the crossflow-plate and uninterrupted-fin core is shown in figure 5. The regenerator is annular in shape with uninterrupted fins in both the air and gas passages. The air and the gases flow straight through the uninterrupted finned passages, as shown in figure 5.

In the design calculations, the regenerator dimensions were calculated by the following procedure: For a series of preassigned gas pressure drops and core inside radii r, the dimensions L and H were computed to give a warming effectiveness of 0.5; the resultant air pressure drops were then computed. The plate spacing for both the air and gas passages was kept constant at 1/4 inch. When the core inside radius was varied, the number of passages N was varied to fill the available space on the core inner circumference. The fin spacing was kept constant at 1/4 inch and fin thicknesses of 0.005 and 0.006 inch and a plate thickness of 0.01 inch were considered.

Crossflow-tubular core. - A schematic diagram of the crossflow-tubular regenerator, which is assumed to be annular in shape, is shown in figure 6. The tubes are located at the vertices of equilateral triangles; the gas flows through the tubes and the air flows across the tubes.

In the design calculations, the core outside diameter was assumed to be 37 inches and the core inside diameter, the tube outside diameter, and the ratio of pitch-to-tube diameter were varied independently. For each set of values of the core parameters, regenerator length and resultant pressure drops were computed for prescribed warming effectivenesses of 0.3 and 0.5.

Counterflow-tubular core. - A schematic diagram of the counterflow-tubular regenerator is shown in figure 7. The counterflow-tubular regenerators were assumed to be ordinary tube bundles with the gas flowing through the tubes and the air along the outside of the tubes.

In the design calculations, the frontal area of the basic core was varied to provide a range of the sum of air and gas pressure drop ratios $(\Delta P/P)_{\Sigma}$ from 0.005 to 0.10 for preassigned warming effectivenesses of 0.5 and 0.75. The only restriction placed on the core was that the flow areas in the air and gas passages be equal. Tube inside diameters of 1/4 and 3/8 inch were considered.

Regenerator-Design Relations

The heat-transfer and pressure-drop formulas used in the regenerator-design calculations are presented in appendix C. The occurrence of pressure drops in the regenerator decreases the engine power and hence increases the specific fuel consumption and specific weight of the regenerated engine to values greater than those resulting with regenerators of zero weight and pressure drop.

The effects of fluid pressure drops on engine specific power and fuel consumption were computed from the cycle analysis. The core weights were calculated by considering all the metal present; a metal density of 0.301 pound per cubic inch was used. The regenerator shell, in every case, was assumed to weigh 35 percent of the core. The weight of ducting to and from the regenerators was not taken into account. In all cases, the regenerators for sea level and 30,000 feet were designed separately for operation at the respective altitudes.

RESULTS AND DISCUSSION

Cycle Analysis

The condition for good load-range performance is a combination of low specific fuel consumption, low specific engine weight, and high power per pound of air per second. Values of these performance parameters for turbine-propeller engines at sea level and 30,000 feet, for combustion temperatures of 1600° and 2500° F, and for a flight speed of 300 miles per hour are shown in figure 8 for a range of compressor pressure ratios and regenerator warming effectivenesses, assuming zero regenerator pressure drops. Also shown are calculated specific weights of unregenerated engines.

In figure 9, the effects of regenerator pressure drops on engine power and thrust specific fuel consumption are shown. The effects of pressure drop at other operating conditions are similar to those indicated in figure 9.

The following conclusions are indicated from figures 8 and 9:

1. For the turbine-propeller engine, the power loss inherent in ideal regeneration (regenerators of zero weight and zero fluid pressure drops) is small.

2. For all regenerator warming effectivenesses between 0.3 and 0.75, the compressor pressure ratios that give approximately minimum specific fuel consumption and maximum power per pound of air per

second with low basic engine weights are as follows:

T (°F)	Altitude (ft)	Compressor pressure ratio
1600	0	6
1600	30,000	8.5
2500	30,000	22

The regenerator cores were designed for this analysis at the pressure ratios presented in the preceding table.

3. Regeneration should not be considered at compressor pressure ratios as high as the following:

T (°F)	Altitude (ft)	Compressor pressure ratio
1600	0	14
1600	30,000	20
2500	30,000	46

4. The ratio $\Delta P/P$ is a convenient measure of loss of engine performance due to pressure drop. With each value of $\Delta P/P$, a definite power loss and a definite increase in specific fuel consumption are associated, irrespective of whether $\Delta P/P$ is for air, for gas, or for the summation of both. The air and the gas pressure drops cause equal losses in engine performance when the ratio of these pressure drops equals the ratio of the respective inlet pressures.

Ideal Gains from Regeneration

The ideal gain from regeneration is defined as the increase in cargo capacity resulting from hypothetical regenerators of zero weight and pressure drop. This value is the upper limit on the gain that may be hoped for from regeneration. The ideal regenerative gains are obtainable from figure 10, which combines in a single plot the cycle-analysis results (presented in fig. 8) with the results of the load-range analysis. In figure 10, the specific weights assignable to engine plus cargo, as given by the load-range analysis, are plotted

as dashed lines against engine thrust specific fuel consumptions for various flight distances. The dashed-line plot in figure 10 can thus be considered as a load-range coordinate plot on which the specific weight and fuel consumption of an engine, as given by the cycle analysis, can be spotted for any specified operating condition. The cargo capacity per engine thrust power is then the difference between the specific weight assignable to engine plus cargo and the engine specific weight for the given engine specific fuel consumption and any assigned flight distance.

On the load-range coordinate plot of figure 10, the engine specific weight and thrust specific fuel consumption for various compressor pressure ratios and warming effectivenesses of the ideal regenerator are presented. For each regenerator warming effectiveness, solid curves are drawn joining the points for the various compressor pressure ratios. The effectiveness values covered in figure 10 are 0, 0.30, 0.50, 0.75, and 0.90; the values of compressor pressure ratio are indicated on the solid curves.

Presentation of the cycle-analysis and weight-estimate results on load-range coordinate plots (as in fig. 10) enables quick evaluation of cargo capacity and optimum compressor pressure ratio for any flight distance and regenerator warming effectiveness. Such an evaluation was made for the case of ideal regeneration for flight speeds of 218, 300, and 400 miles per hour, combustion temperatures of 1600° and 2500° F, altitudes of sea level and 30,000 feet, and flight distances up to 9000 miles. Some of the results of this evaluation are presented in figure 11, from which the effects of variations in warming effectiveness, combustion temperature, flight speed, and flight distance on the gains in cargo capacity resulting from ideal regeneration can be obtained.

From figures 10 and 11 and from additional results of the analysis, the following trends are tabulated:

Increase in	Resultant effect on		
	Optimum compressor pressure ratio	Cargo capacity (lb/thp)	Ideal gain obtainable from regeneration (lb/thp)
Regenerator effectiveness	Decreases	Increases	Increases
Combustion temperature	Increases	Increases	Decreases
Altitude	Increases	Increases	Decreases
Flight speed	Decreases slightly	Decreases	Decreases
Range	Increases	Decreases	Increases

The optimum compressor pressure ratios on the basis of airplane load-range performance at a regenerator warming effectiveness of 0.50 are as follows:

Altitude (ft)	T ($^{\circ}$F)	Optimum compressor pressure ratio
0	1600	6
30,000	1600	8.5
30,000	2500	20

For a combustion temperature of 1600° F, the tabulated compressor pressure ratios for a regenerator warming effectiveness of 0.50 are the same as those estimated from the cycle analysis; for a combustion temperature of 2500° F, the true optimum value (20) is slightly different from the value estimated from the cycle analysis (22).

Actual Gains from Regeneration

The ideal gains from regeneration, shown in figure 11, are the upper limit on the gains that may be hoped for from regeneration. Actual regenerative gains will always be smaller because of the added weight of the regenerator and the fluid pressure drops in the regenerator, which increase engine specific weight and fuel consumption. Accurate evaluation of the gains thus requires consideration of the design of the regenerator core.

Many regenerator designs were made utilizing the core types shown in figures 4 to 7. The range of core dimensions investigated for each core type are given in table I. For each regenerator design, the specific weight and the specific fuel consumption of the regenerative engine operating at the optimum compressor pressure ratio

were calculated. On the basis of these calculations, the optimum designs for each of the core types investigated were selected.

On the load-range coordinate plot of figure 12, the optimum designs of each of the three core types investigated are compared at sea level for a regenerator warming effectiveness of 0.50. Any point along each of the solid curves represents a definite core geometry. The crossflow-tubular core resulted in power losses that were too high for aircraft regenerative application and hence, the final results for this core are not presented herein.

Curve aa of figure 12 is for a series of designs of crossflow-plate and interrupted-fin regenerators (fig. 4). The series resulted from a variation of fin transverse spacing from 0.125 to 0.500 inch, for a fixed air-passage plate spacing of 0.1875 inch, a gas-passage plate spacing of 0.132 inch, and a fin thickness of 0.005 inch. Curve bb is for a set of crossflow-plate and uninterrupted-fin regenerators (fig. 5). This set consists of the optimum cores from several series; the members of any one series were so close to each other in performance that only the optimum core of each series was plotted. Curve cc is for a series of designs of counterflow-tubular regenerators having tubes of 1/4-inch inside diameter (fig. 7). The series resulted from variation of the over-all value of $\Delta P/P$, a procedure equivalent to a wide variation of core outside diameter for a fixed inside diameter of zero.

The curves show that the three core types differ little in performance, hence, any conclusions drawn concerning the effects of the optimum crossflow-plate and interrupted-fin cores will also be valid for the other core types investigated. The slight superiority of the crossflow-plate and interrupted-fin cores implies that the gains from the optimum cores of this type will be a good measure of the gains derivable from regeneration. The characteristics of the crossflow-plate and interrupted-fin core are discussed in detail in appendix D.

In order to determine the actual gains from regeneration, the following designs were selected from among the crossflow-plate and interrupted-fin cores, which are shown in figure 12 to be the best of the cores investigated:

Altitude (ft)	η_R	T (°F)	a (in.)	b (in.)	s (in.)	δ (in.)
0	0.50	1600	0.1875	0.132	0.125 - .500	0.005
30,000	0.30	1600	0.375	0.310	0.125 - 1.00	0.005
	.50		.250	.252	.125 - .500	
	.75		.125	.195	.075 - .500	
	0.30	2500	0.250	0.435	0.125 - .750	0.005
	.50		.250	.252	.125 - .600	
	.75		.125	.195	.125 - .500	

In figure 13, the performance of these cores is presented for a flight speed of 300 miles per hour at 30,000 feet. A straight line parallel to the line of desired flight distance and tangent to the curve of specific weight of the engines with a core series installed determines the optimum core and maximum cargo capacity for the desired flight distance.

A plot such as that in figure 13 gives only cargo capacity; the gain from regeneration as compared with operation at the optimum compressor pressure ratio for the unregenerated engine must be computed by comparison with the cargo capacities calculated for the unregenerated engines operating at their optimum compressor pressure ratios. Gains for flight speeds of 218, 300, and 400 miles per hour, for several flight ranges, and for combustion temperatures of 1600° and 2500° F at sea level and 30,000 feet have been evaluated for the best-designed cores and are presented in table II. The following table presents the largest gains of those listed in table II. The dimensions and the weights of the cores that gave the indicated regenerative gains are presented in appendix D.

Altitude (ft)	T (°F)	η_R	v_0 (mph)	R (miles)	Increase in cargo capacity due to regeneration (lb/thp)	Increase in cargo capacity due to regeneration (lb/ton airplane gross weight)
0	1600	0.50	218	3000	0.51	36
			218	5000	.90	64
			300	3000	.38	56
			400	1000	-.10	-32
30,000	1600	0.50	218	6000	0.35	26
			300	6000	.32	28
			400	3000	-.05	-7
	2500	0.50	218	9000	0.49	38
			300	8000	.38	34
			400	5000	.14	20

The following conclusions are indicated from table II:

1. Maximum gain from regeneration is obtained at a regenerator warming effectiveness of about 0.5. (Cores of the type investigated are too heavy for effectivenesses of 0.75.)

2. For a fixed combustion temperature and regenerator-core type, the gain from regeneration increases as flight distance increases and as altitude and flight speed decrease.

3. The main conclusion from table II is that unless flight is at low speed (about 300 mph) and extends for 3000 or more miles at altitudes near sea level, the gains from regeneration are small. The actual gains are about one-third to one-half of the gains computed for regenerators of zero weight and pressure drop and would be even smaller if weight and pressure drops introduced by ducts leading to and from the regenerator were considered. (Duct weights and pressure drops were neglected in this analysis.)

SUMMARY OF RESULTS

The following results were obtained from an engine-weight and cycle analysis for compressor pressure ratios up to 50, combustion temperatures of 1600° and 2500° F, altitudes of 0 and 30,000 feet, and regenerator warming effectivenesses up to 0.90; from a solution of the load-range equation for flight speeds of 218, 300, and 400 miles per hour and for flight distances up to 9000 miles; and from extensive design calculations for regenerator cores of four types:

1. The maximum gain from regeneration for the core types investigated was obtained with a regenerator warming effectiveness of about 0.5. The optimum compressor pressure ratios on the basis of airplane load-range performance at this warming effectiveness were:

Altitude (ft)	Combustion temperature (°F)	Optimum compressor pressure ratio
0	1600	6
30,000	1600	8.5
30,000	2500	20

2. The gains from regeneration were small except for flights of 3000 miles or more at altitudes near sea level at flight speeds of about 300 miles per hour. The following table presents the largest gains computed in the analysis:

Altitude (ft)	Combustion temperature (^{o}F)	Regenerator warming effectiveness	Flight speed (mph)	Flight distance (miles)	Increase in cargo capacity due to regeneration (lb/thp)	Increase in cargo capacity due to regeneration (lb/ton airplane gross weight)
0	1600	0.50	218	3000	0.51	36
			218	5000	.90	64
			300	3000	.38	56
			400	1000	-.10	-32
30,000	1600	0.50	218	6000	0.35	26
			300	6000	.32	28
			400	3000	-.05	-7
	2500	0.50	218	9000	0.49	38
			300	8000	.38	34
			400	5000	.14	20

The gains tabulated were one-third to one-half of those calculated for regenerators of zero weight and pressure drop and would have been smaller if weights and pressure drops introduced by ducts leading to and from the regenerators had been considered.

Lewis Flight Propulsion Laboratory,
National Advisory Committee for Aeronautics,
Cleveland, Ohio, January 26, 1950.

APPENDIX A

SYMBOLS

Load-Range Designations

The following symbols are used in the load-range equations:

A	effective aspect ratio (in this analysis, A=10)
a	tankage factor
C_V	viscous drag coefficient (in this analysis, C_V=0.025)
D	drag, lb
L	lift, lb
R	flight distance, miles
S	wing surface, sq ft
thp	thrust horsepower
tsfc	thrust specific fuel consumption, lb/thp-hr
v	airplane speed, ft/sec
W	weight, lb
θ	parameter, $\mathrm{thp}\Big/\left(\frac{C_V S\rho}{2}\right)$, $(\mathrm{ft/sec})^3$
ρ	mass density of ambient air, slugs/cu ft

Subscripts:

c	cargo
e	engine
f	fuel
g	gross
s	structure
0	initial

Heat-Transfer, Pressure-Drop, and Core-Variable Designations

The following symbols are used in the heat-transfer and pressure-drop equations and in the designation of core variables:

a	plate spacing in air passage, in. (figs. 4 and 5)
b	plate spacing in gas passage, in. (figs. 4 and 5)
c_p	specific heat of fluid at constant pressure, Btu/(lb)($^\circ$F)
D	outside diameter of tube, ft
d	hydraulic diameter of flow passage, ft
f	friction factor
G	weight flow per unit area, lb/(sec)(sq ft)
g	acceleration of gravity, ft/sec^2
H	width of core, in. (figs. 4 to 6)
h	heat-transfer coefficient, Btu/(sec)(sq ft)($^\circ$F)
k	thermal conductivity, Btu/(sec)(ft)($^\circ$F)
L	length of flow passage, ft or in., as specified (figs. 4 to 6)
N	number of passages of width a (or of width b) or number of plates (figs. 4 and 5)
P	pressure of fluid at entrance to regenerator, lb/sq ft absolute
ΔP	pressure drop of fluid, lb/sq ft
$\left(\frac{\Delta P}{P}\right)_\Sigma$	sum of air and gas pressure-drop ratios, $(\Delta P/P)_a + (\Delta P/P)_g$
Pr	Prandtl number, $c_p\mu/k$
p	center-to-center spacing (pitch) of tubes in crossflow-tubular regenerator, ft (fig. 6)

r	core inside radius (figs. 4 to 6)
S	heat-transfer surface, sq ft
s	transverse spacing between fins, in. (figs. 4 and 5)
T	combustion temperature, $^{\circ}F$
t_w	wall thickness of basic heat-transfer metal, in.
U	over-all heat-transfer coefficient, Btu/(sec)(sq ft)($^{\circ}F$)
W	fluid weight flow, lb/sec
w_R	regenerator weight, lb/(lb air/sec)
δ	thickness of fin metal, in. (figs. 4 and 5)
η_f	fin effectiveness
η_R	regenerator warming effectiveness
ϕ	function of regenerator warming effectiveness, fluid flows, and fluid specific heats
λ	length of strip fin in direction of fluid flow, ft
μ	absolute fluid viscosity, lb/(sec)(ft)
ρ	weight density, lb/cu ft
σ	wall-to-wall spacing of tubes in crossflow-tubular regenerator, in. (fig. 6)
Ψ	mean perimeter of turbine blade, ft

Subscripts:

a	air
av	average
en	entrance
ex	exit
f	fin

g	gas
max	maximum
s	static
t	total
w	basic wall

APPENDIX B

LOAD-RANGE PERFORMANCE EQUATIONS

The weight assignable to engine and cargo for preassigned engine-regenerator combination, initial flight speed, altitude, and flight distance is calculated as follows for a flight plan of constant horsepower and altitude:

$$W_g = (W_e+W_c)+(W_s+aW_f)$$

$$\frac{W_e+W_c}{thp} = \frac{W_g}{thp}\left(1 - \frac{W_s}{W_g} - \frac{aW_f}{W_g}\right)$$

From the definition of L/D for level flight,

$$\frac{W_g}{thp} = \frac{550W_g}{D_0v_0} = \frac{550(L/D)_0}{v_0}$$

where $(L/D)_0$ can be written as follows:

$$\left(\frac{L}{D}\right)_0 = \sqrt{\frac{\pi A}{C_v}}\left[\left(\frac{\rho}{2}\frac{S}{W_g}v_0^2\right)\frac{\sqrt{C_v\pi A}}{1+\left(\frac{\rho}{2}\frac{S}{W_g}v_0^2\right)^2(C_v\pi A)}\right]$$

In this analysis, W_s/W_g is assumed to be 0.4 and the weight of the fuel tanks is taken as $0.1W_f$ so that a is 1.1; the effective aspect ratio A is assumed to be 10; the viscous-drag coefficient C_v is taken as 0.025; and the wing loading W_g/S is constant at 70. These values are typical of current efficient cargo planes.

The following formulas developed in an analysis by the Lewis laboratory are used to calculate W_f/W_g:

$$\frac{R \times tsfc}{375(L/D)_0} = \frac{2}{3}\left[1-\sqrt{\frac{\frac{v^3}{\theta}\left(1-\frac{v^3}{\theta}\right)}{\frac{v_0^3}{\theta}\left(1-\frac{v_0^3}{\theta}\right)}}\right] + \frac{1}{3}\,\frac{\arcsin\sqrt{\frac{v^3}{\theta}} - \arcsin\sqrt{\frac{v_0^3}{\theta}}}{\sqrt{\frac{v_0^3}{\theta}\left(1-\frac{v_0^3}{\theta}\right)}}$$

and

$$\frac{W_f}{W_g} = 1-\sqrt{\left(\frac{v}{v_0}\right)\frac{\left(1-\frac{v^3}{\theta}\right)}{\left(1-\frac{v_0^3}{\theta}\right)}}$$

For this flight plan, the velocity increases as time of flight increases; the flight speeds presented herein are the initial values.

APPENDIX C

HEAT-TRANSFER AND PRESSURE-DROP FORMULAS

Heat-Transfer Relations

The over-all conductance US required to produce a desired regenerator warming effectiveness η_R for assigned fluid flows and known specific heats is functionally expressed by

$$US = \phi[\eta_R, (Wc_p)_a, (Wc_p)_g]$$

This relation is given in reference 6 for single-pass crossflow heat exchangers in which neither fluid is mixed. For a single-pass crossflow heat exchanger in which one of the fluids is mixed, this relation, which is obtained by a series solution of the basic differential equations by a method similar to that of reference 6, is plotted in figure 14; this relation was used in the design calculations of the crossflow-tubular regenerator core shown in figure 6.

The value of US is also expressed by the equation

$$US = \frac{(hS)_a(hS)_g}{(hS)_a+(hS)_g}$$

The right member of this equation involves the dimensions of the heat-exchanger core, and when equated to the numerical value of US obtained from the functional relation ϕ, a design equation is obtained.

The formula for the heat-transfer coefficient in turbulent flow through a smooth passage is the standard Nusselt correlation

$$\frac{hd}{k} = 0.023\left(\frac{c_p\mu}{k}\right)^{0.4}\left(\frac{Gd}{\mu}\right)^{0.8}$$

The formula (from reference 7) employed for the heat-transfer coefficient in flow through a passage having interrupted-strip fins is

$$\left(\frac{h}{c_p G}\right)Pr^{2/3} = 0.60\sqrt{\left(\frac{\lambda}{d}\right)\left(\frac{Gd}{\mu}\right)} \quad \text{for } \lambda/d \leq 3.5$$

$$= 0.60\sqrt{3.5\left(\frac{Gd}{\mu}\right)} \quad \text{for } \lambda/d > 3.5$$

For the radial-crossflow-tubular regenerator, the heat-transfer coefficient of the shell side is calculated by the heat-transfer correlation for turbulent flow across banks of tubes (reference 8, p. 229, equation 8).

$$\frac{hD}{k} = 0.33\left(\frac{c_p\mu}{k}\right)^{1/3}\left(\frac{G_{max}D}{\mu}\right)^{0.6}$$

For the counterflow-tubular regenerators, the standard Nusselt correlation for flow through smooth tubes is used.

The effective heat-transfer surface in an unfinned passage is the actual wall surface. The effective surface in a finned passage is the sum of the wall surface and the fraction of the fin surface that is effective for heat transfer:

$$S = \left(S_w + \eta_f S_f\right)$$

The formula for η_f is given by the right member of equation (10a), page 232, of reference 8.

Pressure Relations

The relation employed to calculate the total-pressure drop is

$$\Delta P_t = \Delta P_s - \left(\frac{G^2}{2g}\right)\left(\frac{1}{\rho_{ex}} - \frac{1}{\rho_{en}}\right)$$

By substituting in the preceding equation the following equivalent of ΔP_s

$$\Delta P_s = f\left(\frac{G^2}{2\rho_{av}g}\right)\left(\frac{4L}{d}\right) + \left(\frac{G^2}{g}\right)\left(\frac{1}{\rho_{ex}} - \frac{1}{\rho_{en}}\right)$$

the following relation is obtained:

$$\Delta P_t = f\left(\frac{G^2}{2\rho_{av}g}\right)\left(\frac{4L}{d}\right) + \left(\frac{G^2}{2g}\right)\left(\frac{1}{\rho_{ex}} - \frac{1}{\rho_{en}}\right)$$

The expressions for f for turbulent flow through tubes and across banks of staggered tubes are available in reference 8, page 119, equation (9a), and page 126, equation (19a), respectively. The formula for f in a passage with interrupted fins is obtained from reference 7. The friction factor for interrupted fins shows a transition at Gd/μ of 3500; hence two equations are used. For $Gd/\mu \leq 3500$

$$f = \frac{11.8}{(\lambda/d)}\left(\frac{Gd}{\mu}\right)^{-0.67} \quad \text{for} \quad \lambda/d \leq 3.5$$

which, becomes

$$f = \frac{11.8}{3.5}\left(\frac{Gd}{\mu}\right)^{-0.67} \quad \text{for} \quad \lambda/d > 3.5$$

For $Gd/\mu > 3500$

$$f = \frac{0.38}{(\lambda/d)}\left(\frac{Gd}{\mu}\right)^{-0.24} \quad \text{for} \quad \lambda/d \leq 3.5$$

which becomes

$$f = \frac{0.38}{3.5}\left(\frac{Gd}{\mu}\right)^{-0.24} \quad \text{for} \quad \lambda/d > 3.5$$

APPENDIX D

ANALYSIS OF CROSSFLOW-PLATE AND INTERRUPTED-FIN CORE

Effect of core diameters. - The following table shows the most marked effects calculated for substantial variations in core diameters on the load-range performance of a regenerated engine. Inasmuch as the length of the fins does not substantially affect the results due to diameter variations, the conclusions should be valid for plate- and fin-type cores independent of fin interruption.

Altitude (ft)	Core type	η_R	Core O.D. (in.)	Core I.D. (in.)	Specific wt. of engine plus core (lb/thp)	tsfc (lb/ thp-hr)	V_0 (mph)	R (miles)	Cargo capacity (lb/ thp)
0	Crossflow plate and uninterrupted fins	0.50	43.0 43.4	21.4 15.8	1.85 1.77	0.525 .534	300	3000	0.60 .58
			40.6 48.2	15.8	1.79 1.77	0.533 .541	300	3000	0.58 .51
30,000	Crossflow plate and interrupted fins	0.50	44 37	32 26.4	2.55 2.52	0.435 .436	300	6000	1.94 1.95

The data presented in the preceding table show that: For a constant core outside diameter, a 20- to 30-percent variation in core inside diameter produces a negligible effect on cargo capacity; for a constant core inside diameter, a 15- to 20-percent variation in core outside diameter produces a variation in cargo capacity (at the conditions indicated) of less than 0.1 pound per thrust horsepower; and the performance obtained with one set of diameters can be closely reproduced with a substantially different set of diameters. Hence, core diameters are not critical in core design and the optimum core obtained with one reasonably selected set of diameters will not differ substantially from the optimum core obtainable by varying diameters alone.

Effect of plate and fin spacings. - The design calculations showed that for each spacing in the air passage there is a combination of plate spacings and fin transverse spacings in the gas passage that leads to the optimum core and that deviation from the proper spacings in the gas passage can very substantially decrease performance. If the optimum cores for several values of air-passage plate spacings are compared, however, a useful result appears, as shown by the following data for high-performance cores:

Altitude (ft)	Core type	η_R	a (in.)	b (in.)	s (in.)	Specific wt. of engine plus core (lb/thp)	tsfc (lb/ thp-hr)	V_0 (mph)	R (miles)	Cargo capacity (lb/ thp)
30,000	Crossflow plate and interrupted fin	0.50	0.125	0.195	0.375	2.55	0.436	300	6000	1.92
			.1875	.315	.250	2.56	.435			1.93
			.250	.252	.250	2.58	.434			1.93
			.375	.310	.250	2.64	.431			1.93

The table shows that air-passage plate spacing is not critical and that for any reasonable value of this plate spacing, a calculation for several gas-passage plate and fin transverse spacings will determine a combination that does not substantially differ from the optimum performance obtainable with any other reasonable air-passage plate spacing. This conclusion is also true if the gas-passage plate spacing is chosen as the independent parameter.

Effect of ratio of fin length before interruption to passage hydraulic diameter (λ/d). - For interrupted fins, it is of interest to ascertain whether an optimum interruption interval exists. The following data are for a spacing of 0.25 inch between plates in both the air and gas passages and for a fin transverse spacing of 0.25 inch:

Altitude (ft)	η_R	λ/d	Specific wt. of engine plus core (lb/thp)	tsfc (lb/thp-hr)	V_0 (mph)	R (miles)	Cargo capacity (lb/thp)
30,000	0.50	0.50	2.68	0.459	300	6000	1.35
		0.75	2.59	.438			1.84
		1	2.58	.434			1.93
		4	2.70	.429			1.91

The optimum performance occurs at a λ/d of 1 but the deviation from optimum performance is very small for values of λ/d from 0.75 to well beyond unity; hence, for values of λ/d greater than 0.75 the precise value of the ratio is unimportant in load-range performance.

Effect of fin thickness. - An increase in fin thickness increases the effectiveness of the fin for heat conduction but increases core weight and pressure drop. It is therefore of interest to ascertain which effect of fin thickness dominates. The following data are for an air-passage plate spacing of 0.1875 inch, a gas-passage plate spacing of 0.132 inch, and a fin transverse spacing of 0.25 inch. Other spacings show the same effect of fin thickness.

Altitude (ft)	η_R	δ (in.)	Specific wt. of engine plus core (lb/tnp)	tsfc (lb/thp-hr)	V_0 (mph)	R (miles)	Cargo capacity (lb/thp)
0	0.50	0.005	1.45	0.522	300	3000	1.03
		.010	1.51	.523			.96
		.020	1.62	.526			.82

The optimum performance results from the thinnest fins.

The analysis of the design data for the crossflow-plate and interrupted-fin regenerators indicates that for a warming effectiveness of 0.50 there is a single best performance but no one optimum set of core dimensions. Thus, if a design incorporates the minimum practical fin thickness, a value of λ/d of about 1, and a fin transverse spacing of about 0.25 inch, any reasonably selected set of core diameters and air-passage plate spacings can be expected to

to give very nearly best performance of the core type; the optimum gas-passage plate spacing can be determined by assigning a series of values.

Effect of regenerator warming effectiveness. - The following table shows the effect of increasing the regenerator warming effectiveness in an effort to increase the cargo gains from regeneration; the tabulated cores are the best of those designed at the indicated warming effectiveness:

Altitude (ft)	T (°F)	η_R	a (in.)	b (in.)	s (in.)	δ (in.)	t_w (in.)	L (ft)	w_R (lb/(lb air/sec))	Specific wt. of engine plus regenerator (lb/thp)	tsfc (lb/thp-hr)	v_0 (mph)	R (miles)	Cargo capacity (lb/thp)
30,000	1600	0.30	0.375	0.310	0.750	0.005	0.01	2.16	26.5	2.36	0.458	300	6000	1.25
		.50	.250	.252	.250			2.61	44.3	2.58	.434			1.93
		.75	.125	.195	.075			3.50	110.3	3.23	.398			1.97

The preceding table shows that regenerator weight rapidly increases as the warming effectiveness increases and that cargo capacity therefore does not increase rapidly, regardless of the decrease in fuel consumption; hence, no advantage results from designing for an effectiveness beyond about 0.5.

Effect of altitude. - The effect of altitude on the regenerator-core dimensions and on load-range performance is shown in the following table. The tabulated cores are the best of those designed for an effectiveness of 0.50:

Altitude (ft)	T (°F)	η_R	a (in.)	b (in.)	s (in.)	δ (in.)	t_w (in.)	L (ft)	w_R (lb/(lb air/sec))	Specific wt. of engine plus regenerator (lb/thp)	tsfc (lb/thp-hr)	v_0 (mph)	R (miles)	Cargo capacity (lb/thp)
0	1600	0.50	0.1875	0.132	0.250	0.005	0.01	2.27	22.5	1.45	0.521	300	3000	1.05
30,000			.250	.252				2.61	44.3	2.58	.434			6.17

For constant warming effectiveness, core length increases and core weight nearly doubles as altitude increases from 0 to 30,000 feet. At sea level, the power loss due to pressure drop is 1.5 thrust horsepower per pound of air per second, divided equally between air and gas; at 30,000 feet the power loss is 2.5 thrust horsepower per pound of air per second, two-thirds of which results from gas pressure drop. Thus, both weight and power loss are approximately doubled as the altitude increases from 0 to 30,000 feet.

Effect of combustion temperature. - Dimensions and weights of the optimum regenerator cores designed for a combustion temperature of 2500° F are given in the following table:

Altitude (ft)	T (°F)	η_R	a (in.)	b (in.)	s (in.)	δ (in.)	t_w (in.)	L (ft)	w_R (lb/(lb air/sec))	Specific wt. of engine plus regenerator (lb/thp)	tsfc (lb/thp-hr)	V_0 (mph)	R (miles)	Cargo capacity (lb/thp)
30,000	2500	0.30	0.25	0.435	0.625	0.005	0.02	1.75	36.0	2.00	0.392	300	6000	3.30
		.50	.25	.252	.500			3.86	104.2	2.27	.372			3.47
		.75	.125	.195	.125			4.77	214.0	2.78	.354			3.27

The tabulated values show the same general trends with warming effectiveness for combustion temperatures of 2500° and 1600° F. For a constant warming effectiveness, the 2500° F core is heavier than the 1600° F core because the parent metal is increased from 0.01 to 0.02 inch to accommodate the higher compressor pressure ratio at 2500° F. The fin thickness is, however, maintained constant and the core weights are therefore not proportional to the respective core lengths.

Dimensions and weights of optimum regenerator cores. - The size and the weight of the optimum cores vary with warming effectiveness, altitude, combustion temperature, flight distance, and flight speed. For the crossflow-plate and interrupted-fin cores, the size and the weight of the optimum cores are not very sensitive to flight distance, as shown in figures 12 and 13, or to flight speed. The dimensions and the weights of the optimum crossflow-plate and interrupted-fin cores for altitudes, combustion temperatures, warming effectivenesses, and gains from regeneration shown in table II are presented in the following table:

Altitude (ft)	T (^{o}F)	η_R	a (in.)	b (in.)	s (in.)	δ (in.)	t_w (in.)	Core O.D. (in.)	Core I. D. (in.)	L (ft)	w_R (lb/(lb air/sec))
0	1600	0.50	0.1875	0.132	0.250	0.005	0.01	44	32	2.27	22.5
30,000	1600	0.30	0.375	0.310	0.750	0.005	0.01	44	32	2.16	26.5
		.50	.250	.252	.250					2.61	44.3
		.75	.125	.195	.075					3.50	110.3
	2500	0.30	0.25	0.435	0.625	0.005	0.02	44	32	1.75	36.0
		.50	.25	.252	.500					3.86	104.2
		.75	.125	.195	.125					4.77	214.0

The gains from regeneration shown in table II for a regenerator warming effectiveness of 0.75 at sea level were calculated for counterflow-tubular regenerators having tubes of 3/8-inch inside diameter and 0.01-inch wall thickness. The calculation of core weight and power loss due to pressure drops for these regenerators did not require a knowledge of over-all core dimensions, which were therefore not calculated. The weight of the optimum counterflow-tubular core at sea level varied more with flight distance than did the weight of the crossflow-plate and interrupted-fin core and ranged from 138 pounds per pound of air per second for a 3000-mile flight to 165 pounds per pound of air per second for a 6000-mile flight.

REFERENCES

1. Wood, George P.: Analytical Investigation of the Use of Regeneration in Compressor-Turbine-Propeller Systems. NACA RM L6I09, 1946.

2. Trout, Arthur M., and Hall, Eldon W.: Method for Determining Optimum Division of Power between Jet and Propeller for Maximum Thrust Power of a Turbine-Propeller Engine. NACA TN 2178, 1950.

3. Machlin, E. S., and Nowick, A. S.: Stress Rupture of Heat-Resisting Alloys as a Rate Process. NACA TN 1126, 1946.

4. Keenan, Joseph H., and Kaye, Joseph: Thermodynamic Properties of Air. John Wiley & Sons, Inc., 1945.

5. Turner, L. Richard, and Bogart, Donald: Constant-Pressure Combustion Charts Including Effects of Diluent Addition. NACA Rep. 937, 1949. (Formerly NACA TNs 1086 and 1655.)

6. Nusselt, Wilhelm: Eine neue Formel für den Wärmedurchgang im Kreuzstrom. Tech. u. Mech. Thermodynamik, Bd. 1, Nr. 12, Dez. 1930, S. 417-422.

7. Manson, Simon V.: Correlation of Heat-Transfer Data and of Friction Data for Interrupted Plane Fins Staggered in Successive Rows. NACA TN 2237, 1950.

8. McAdams, William H.: Heat Transmission. McGraw-Hill Book C ., Inc., 1942.

TABLE I - RANGES OF REGENERATOR-CORE PARAMETERS INVESTIGATED

(a) Crossflow-plate and interrupted-fin cores (fig. 4).

Altitude (ft)	T (^{o}F)	η_R	Core I.D. (in.)	H (in.)	a (in.)	b (in.)	s (in.)	λ/d	t_w (in.)	δ (in.)
0	1600	0.50	32	6	0.125 .1875	0.12 - .20	0.125 - .500	0.61 - 4.0	0.01 .02	0.005 - .02
30,000	1600	0.30	32	6	0.125 - .375	0.070 - .50	0.125 - 1.00	0.61 - 4.0	0.01 .02	0.005
		0.50	32 26.4	6 5.3		.070 - .92	.125 - .500	.5 - 4.0		
		.75	32	6		0.07 - .50	0.075 - .500	0.6 - 4.0		
	2500	0.30	32	6	0.125 - .375	0.07 - .50	0.125 - 1.0	0.61 - 4.0	0.02	0.005
		.50				.070 - .92	.125 - .750	.5 - 4.0		
		.75				.07 - .50	.125 - .500	.61 - 4.0		

(b) Crossflow-plate and uninterrupted-fin cores (fig. 5).

Altitude (ft)	T (^{o}F)	η_R	Core I.D. (in.)	H (in.)	a (in.)	b (in.)	s (in.)	λ/d	t_w (in.)	δ (in.)
0	1600	0.50	15.8 - 24.1	10.4 - 16.2	0.25	0.25	0.25	144 - 216	0.01	0.006 .005

(c) Crossflow-tubular cores (fig. 6).

Altitude (ft)	T (^{o}F)	η_R	Core O.D. (in.)	Core O.D. (in.)	D (in.)	t_w (in.)	p/D
30,000	1600	0.30	37	6 - 27	0.125 - .375	0.01	1.2 - 2.0
		.50			.125 - .25		

(d) Counterflow-tubular cores (fig. 7).

Altitude (ft)	T (^{o}F)	η_R	Core O.D. (in.)	Core I.D. (in.)	Tube I.D. (in.)	t_w (in.)	$\left(\frac{\Delta P}{P}\right)_\Sigma$
0	1600	0.50 .75	28 - 58	0	0.25 .375	0.01	0.005 - .10
30,000	1600	0.50 .75	28 - 58	0	0.375	0.01	0.01 - .10

TABLE II - CARGO-CAPACITY GAINS CALCULATED FOR REGENERATED ENGINES ASSUMED TO HAVE OPTIMUM REGENERATOR CORES INSTALLED[a]

Altitude (ft)	T (°F)	v_0 (mph)	η_R	H (miles)	Cargo capacity of regenerated engine at optimum compressor pressure ratio (lb/thp)	Cargo capacity of unregenerated engine at optimum compressor pressure ratio (lb/thp)	Actual gain from regeneration (lb/thp)	Actual gain from regeneration (lb/ton airplane gross weight)	Amount of cargo by which actual regenerative gain is less than gain from regenerator of zero weight and pressure drop (lb/thp)
0	1600	218	0.50	3000	7.60	7.09	0.51	56	0.49
				5000	2.72	1.82	.90	64	.57
				6000	.33	----	----	---	----
			0.75	3000	6.91	7.09	[b]-0.18	-13	2.01
				5000	2.49	1.82	[b] .67	48	2.21
				6000	.25	----	----	---	----
		300	0.50	3000	1.05	0.67	0.38	56	0.40
			.75		.20	----	[b].47	-70	1.80
		400	0.50	1000	0.81	0.91	-0.10	-32	0.34
30,000	1600	218	0.30	3000	7.96	7.94	0.02	2	0.30
				6000	3.08	3.05	.03	2	.48
			0.50	3000	8.01	7.94	0.07	5	0.59
				6000	3.40	3.05	.35	26	.69
				8000	.45	----	----	---	----
			0.95	3000	7.73	7.94	-0.21	-16	1.56
				6000	3.40	3.05	.35	26	1.88
				8000	.75	----	----	---	----
		300	0.30	3000	6.14	6.16	-0.02	-2	0.29
				6000	1.68	1.65	.03	3	.44
			0.50	3000	6.17	6.16	0.01	1.0	0.57
				6000	1.97	1.65	.32	28	.85
				7000	.81	.20	.41	38	.87
			0.95	3000	5.97	6.18	-0.29	-26	1.48
				6000	1.97	1.65	.32	28	1.75
				7000	.68	.20	.48	44	----
		400	0.30	3000	2.07	2.10	-0.03	-4	0.38
			.50		2.05		-.06	-7	.57
			.75		1.67		-.43	-64	1.44
	[c]2500	218	0.30	3000	9.06	8.98	0.08	6	0.19
				6000	4.82	4.70	.12	9	.25
				9000	.83	.70	.13	10	.36
			0.50	3000	9.09	8.98	0.11	8	0.39
				6000	5.02	4.70	.32	24	.45
				9000	1.19	.70	.49	38	.45
			0.75	3000	8.81	8.98	-0.17	-13	1.04
				6000	4.89	4.70	.19	14	1.18
				9000	1.17	.70	.47	36	----
		300	0.30	3000	7.17	7.11	0.06	5	0.15
				6000	3.30	3.20	.10	9	.25
				8000	.88	.77	.11	10	.25
			0.50	3000	7.17	7.11	0.06	5	0.40
				6000	3.47	3.20	.27	24	.42
				8000	1.15	.77	.38	34	.42
			0.75	3000	6.76	7.11	-0.35	-32	1.14
				6000	3.27	3.20	.07	6	1.41
				8000	1.06	.77	.28	26	1.24
		400	0.30	3000	2.96	2.94	0.02	3	0.20
				5000	.88	.80	.08	12	.18
			0.50	3000	2.92	2.94	-0.02	-3	0.39
				5000	.94	.80	.14	20	.39
			0.75	3000	2.49	2.94	-0.50	-74	0.89
				5000	.61	.80	-.19	-28	1.16

[a]Regenerator-core dimensions are presented in appendix D.

[b]These values were calculated for counterflow-tubular regenerators and are not strictly comparable with other tabulated values, which were calculated for crossflow-plate and interrupted-fin regenerators.

[c]Regenerator-plate thickness for combustion temperature of 2500° F was twice the thickness for combustion temperature 1600° F.

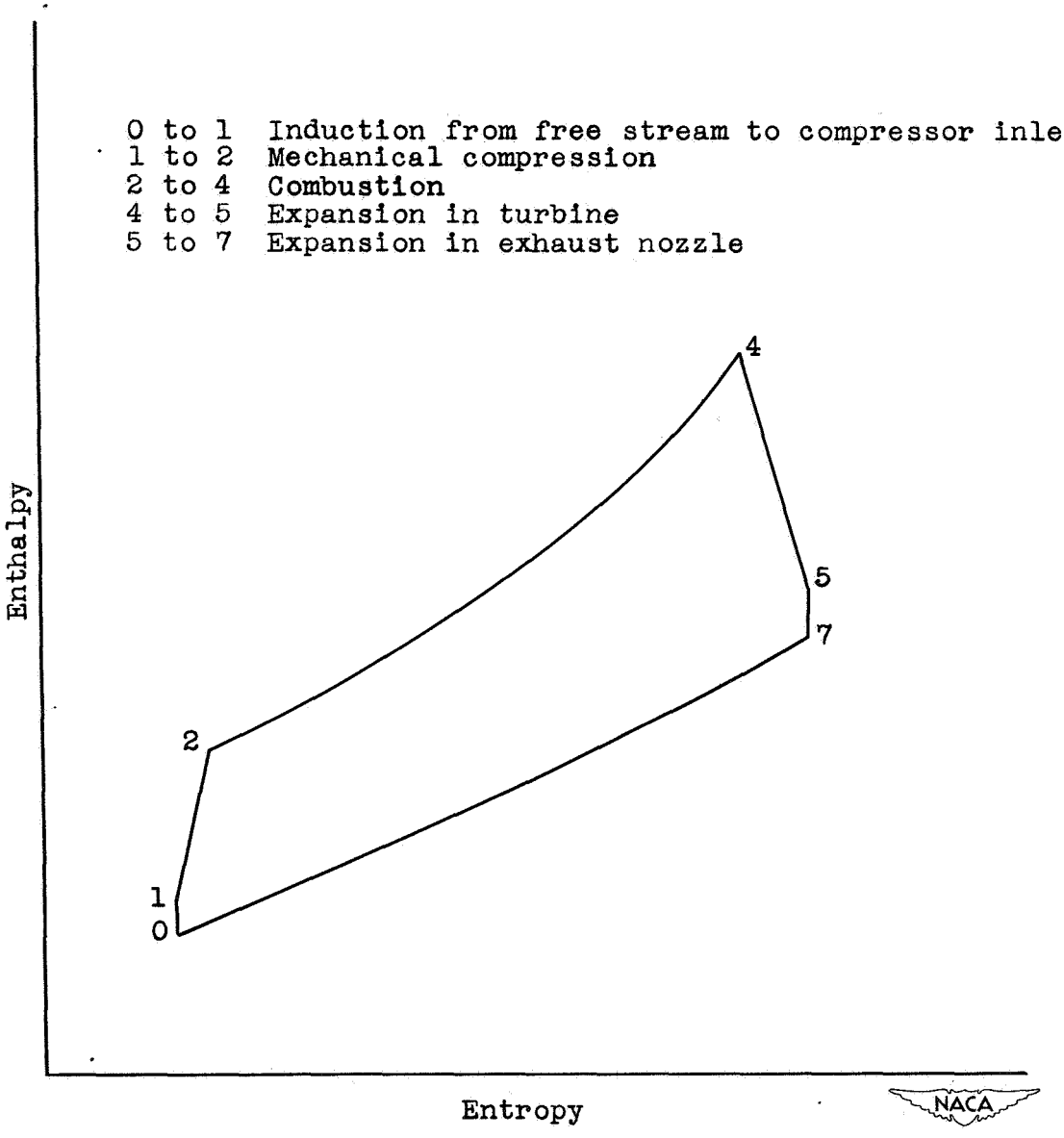

Figure 1. - Unregenerative compressor-turbine cycle.

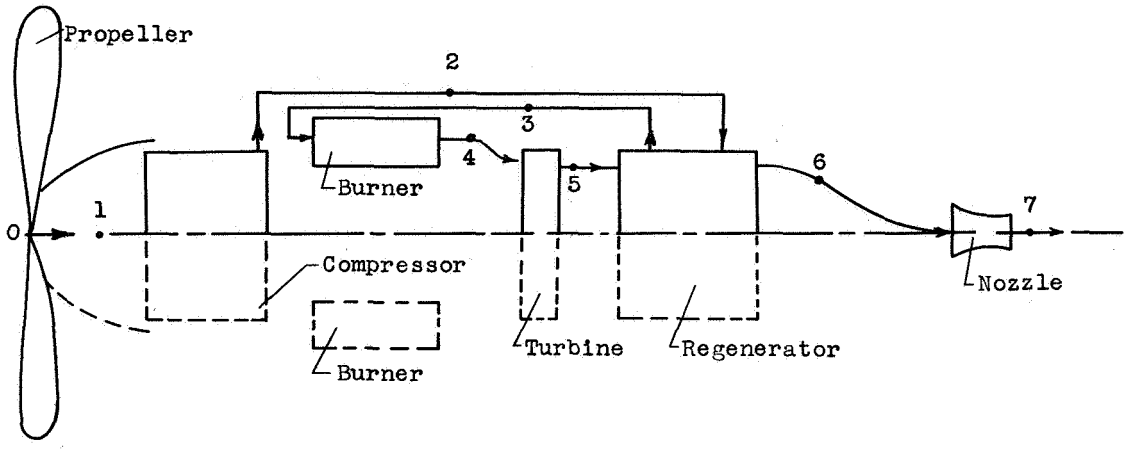

Figure 2. - Regenerative compressor-turbine-propeller power plant.

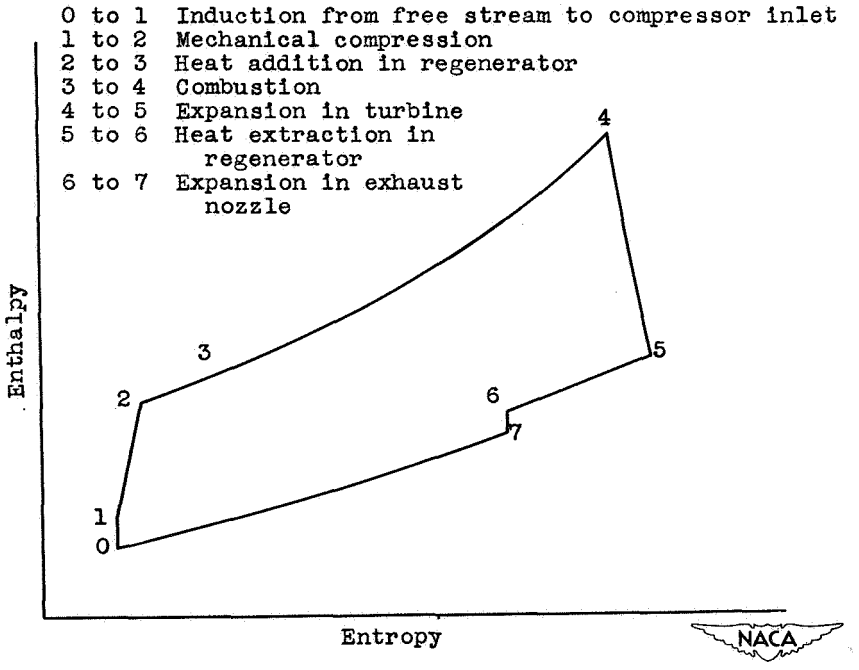

Figure 3. - Regenerative compressor-turbine cycle.

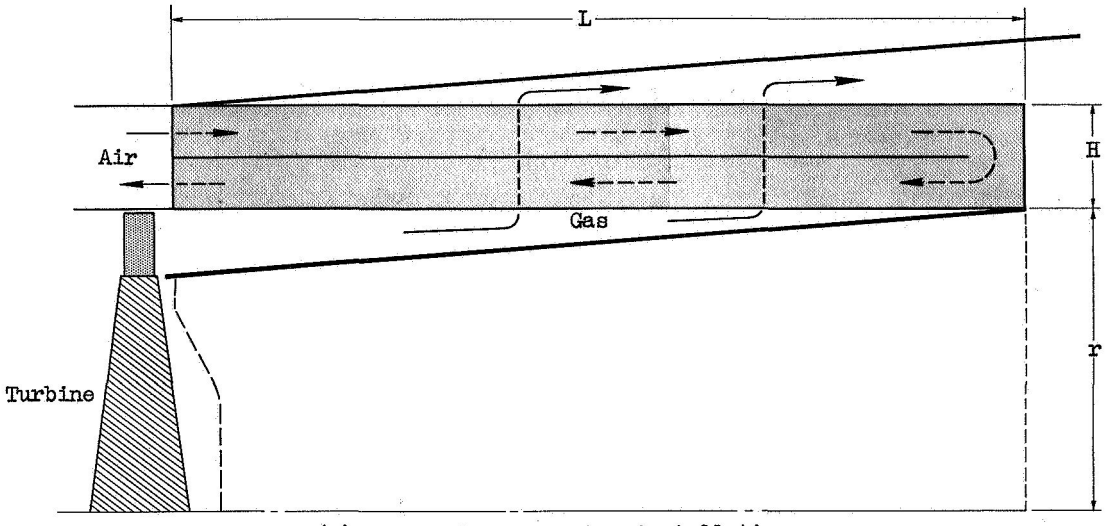

(a) Assumed regenerator installation.

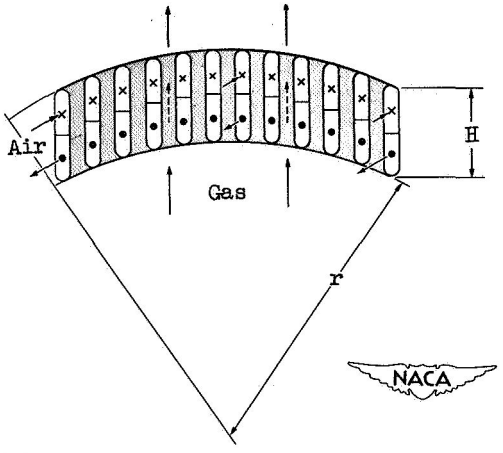

(b) Flow-passage arrangement in segment of regenerator.

Figure 4. - Crossflow-plate and interrupted-fin regenerator with finned gas passages and smooth air passages.

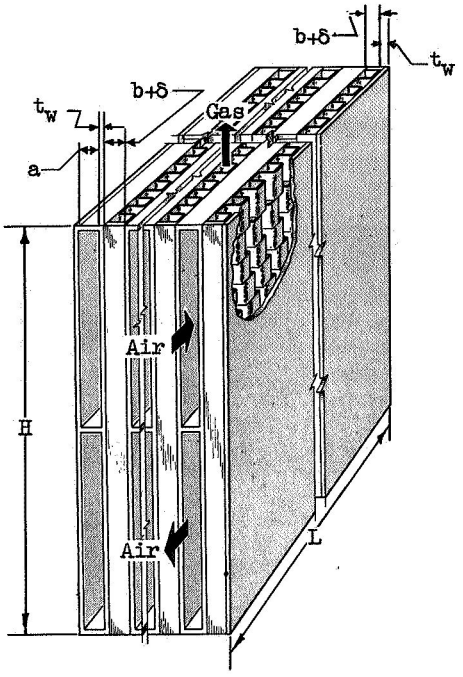

(c) Flow-passage detail.

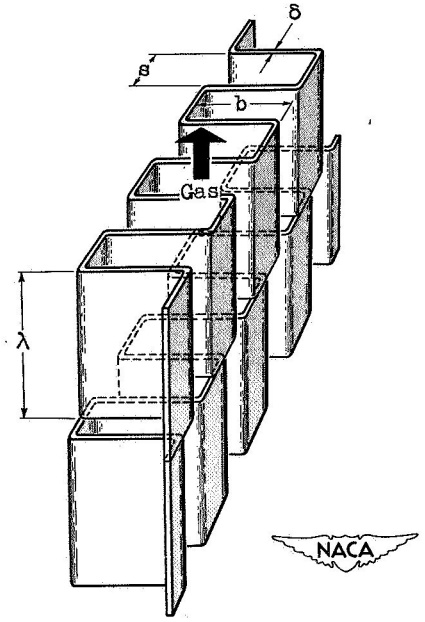

(d) Fin detail in gas passage.

Figure 4. - Concluded. Crossflow-plate and interrupted-fin regenerator with finned gas passages and smooth air passages.

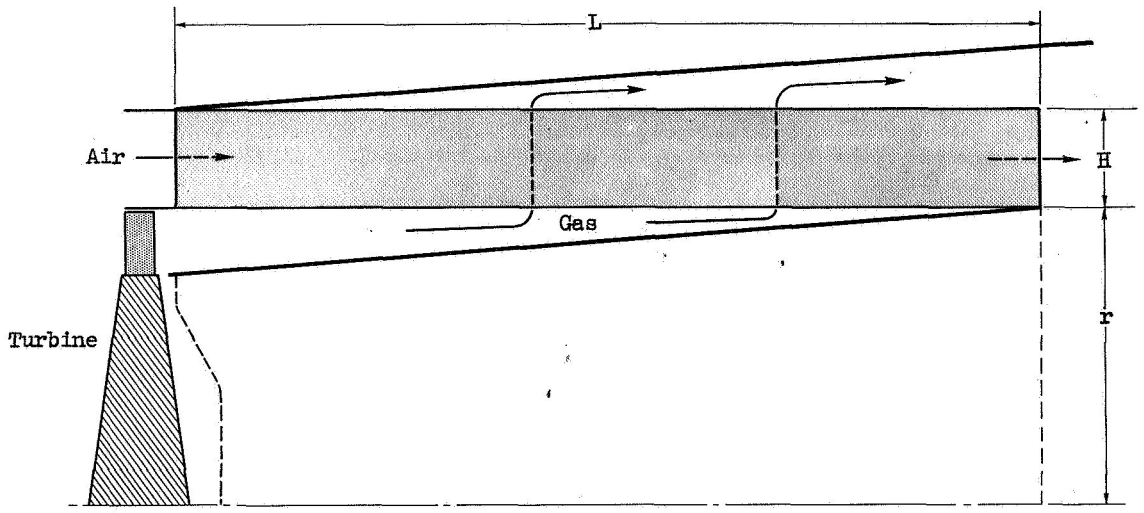

(a) Assumed regenerator installation.

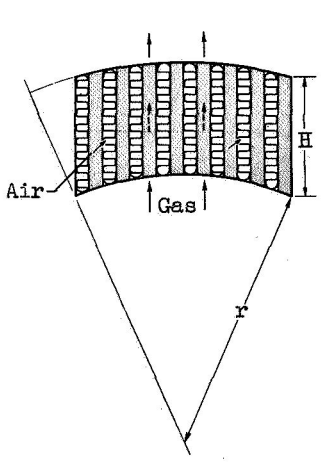

(b) Flow-passage arrangement in segment of regenerator.

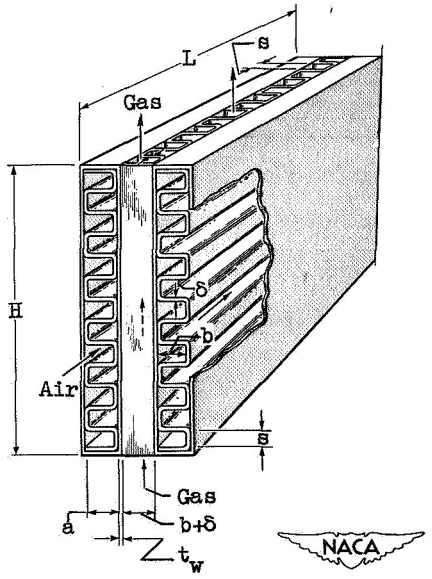

(c) Flow-passage detail.

Figure 5. - Crossflow-plate and uninterrupted-fin regenerator with finned air and gas passages.

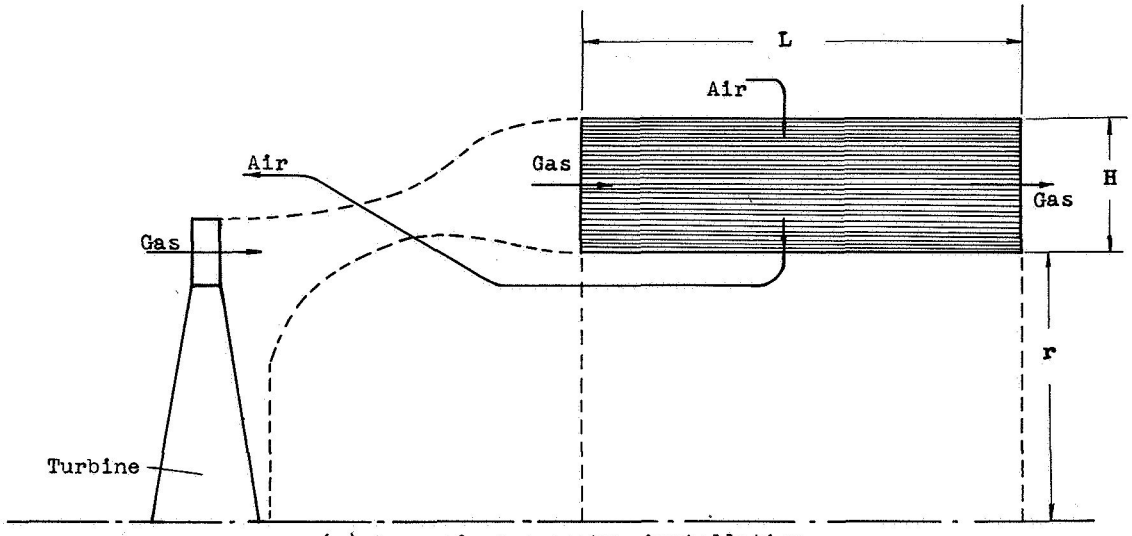

(a) Assumed regenerator installation.

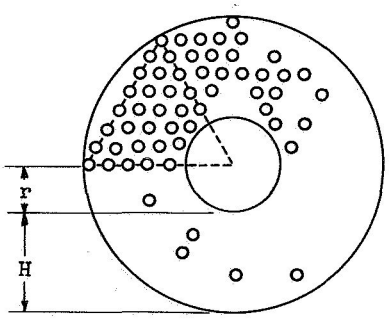

(b) Tube arrangement.

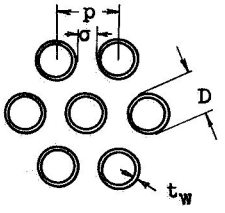

(c) Tube detail.

Figure 6. - Crossflow-tubular regenerator.

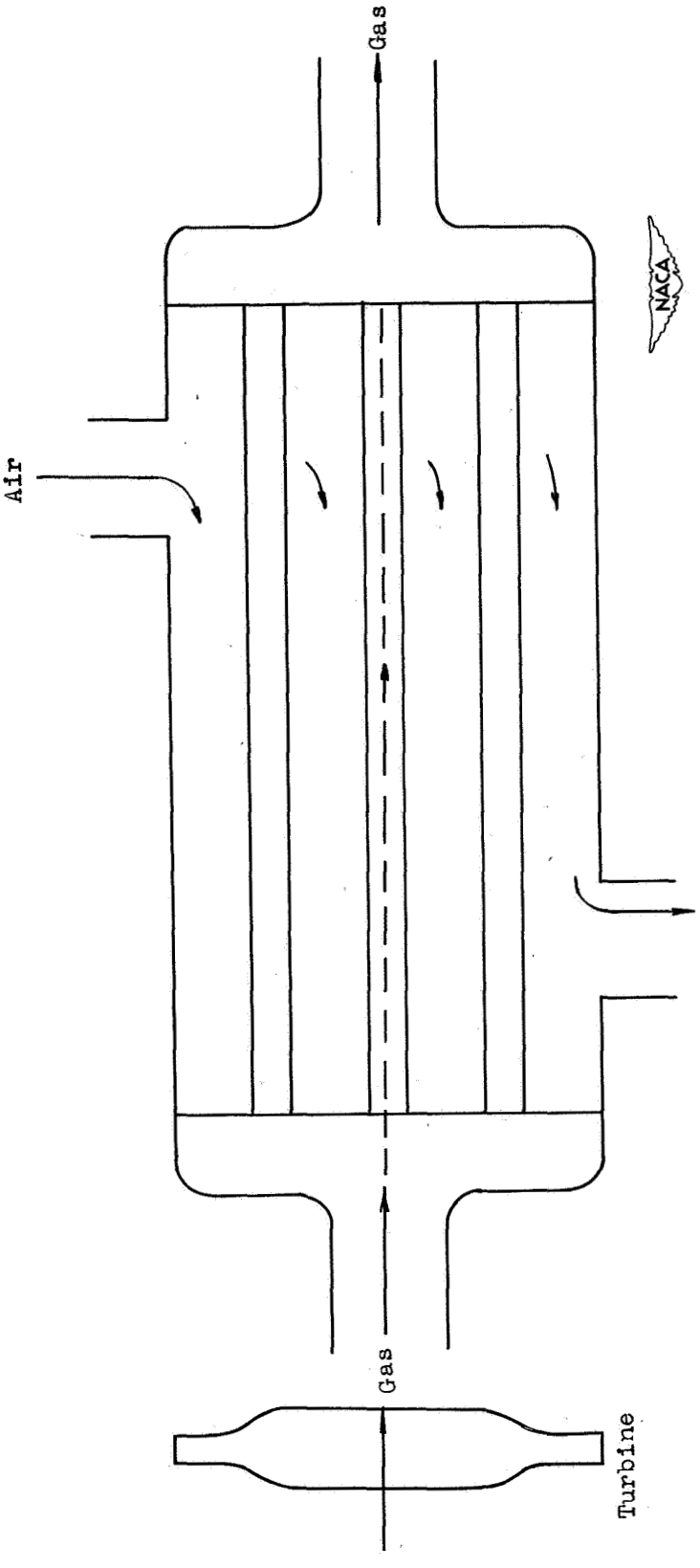

Figure 7. - Schematic diagram of counterflow-tubular regenerator.

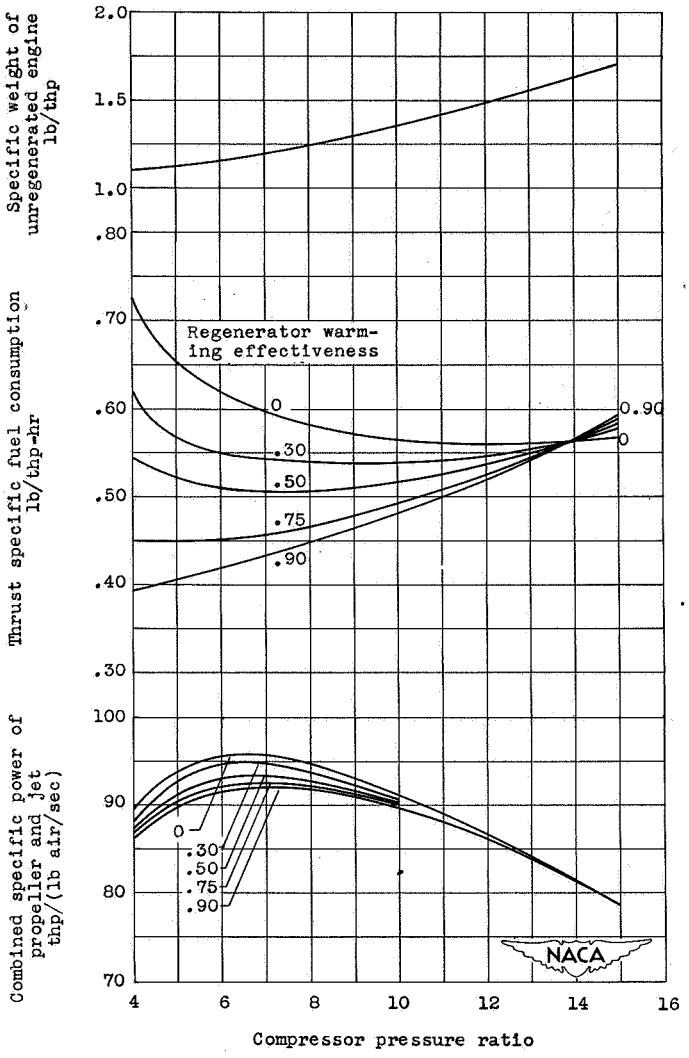

(a) Combustion temperature, 1600° F; altitude, sea level.

Figure 8. - Specific power, thrust specific fuel consumption, and specific weight of turbine-propeller engines at various compressor pressure ratios and regenerator warming effectivenesses. Flight speed, 300 miles per hour; regenerator pressure drops, 0.

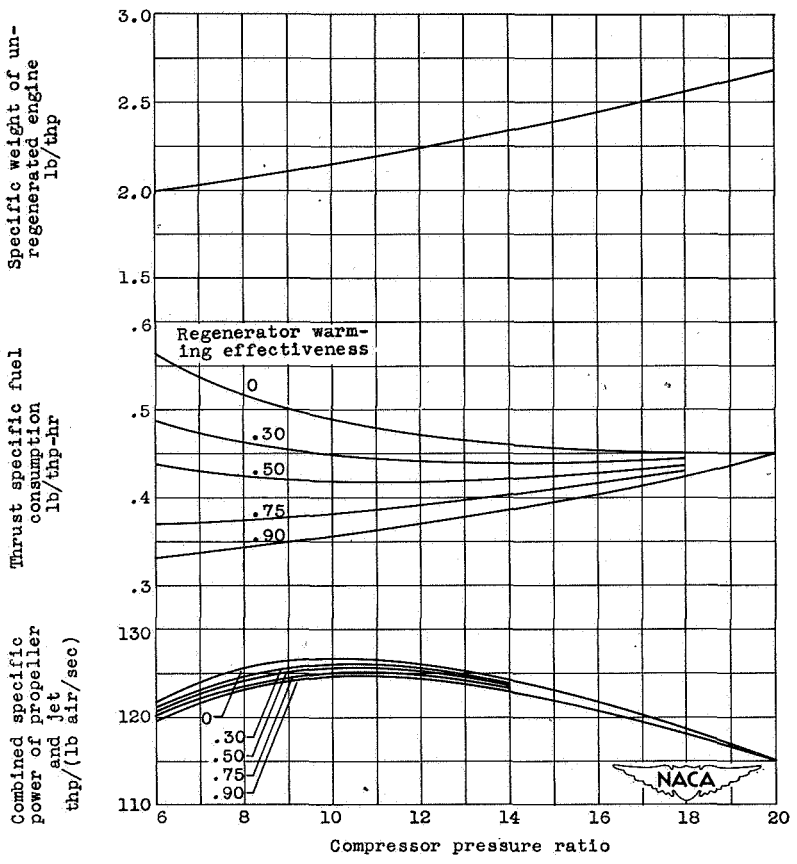

(b) Combustion temperature, 1600° F; altitude, 30,000 feet.

Figure 8. - Continued. Specific power, thrust specific fuel consumption, and specific weight of turbine-propeller engines at various compressor pressure ratios and regenerator warming effectivenesses. Flight speed, 300 miles per hour; regenerator pressure drops, 0.

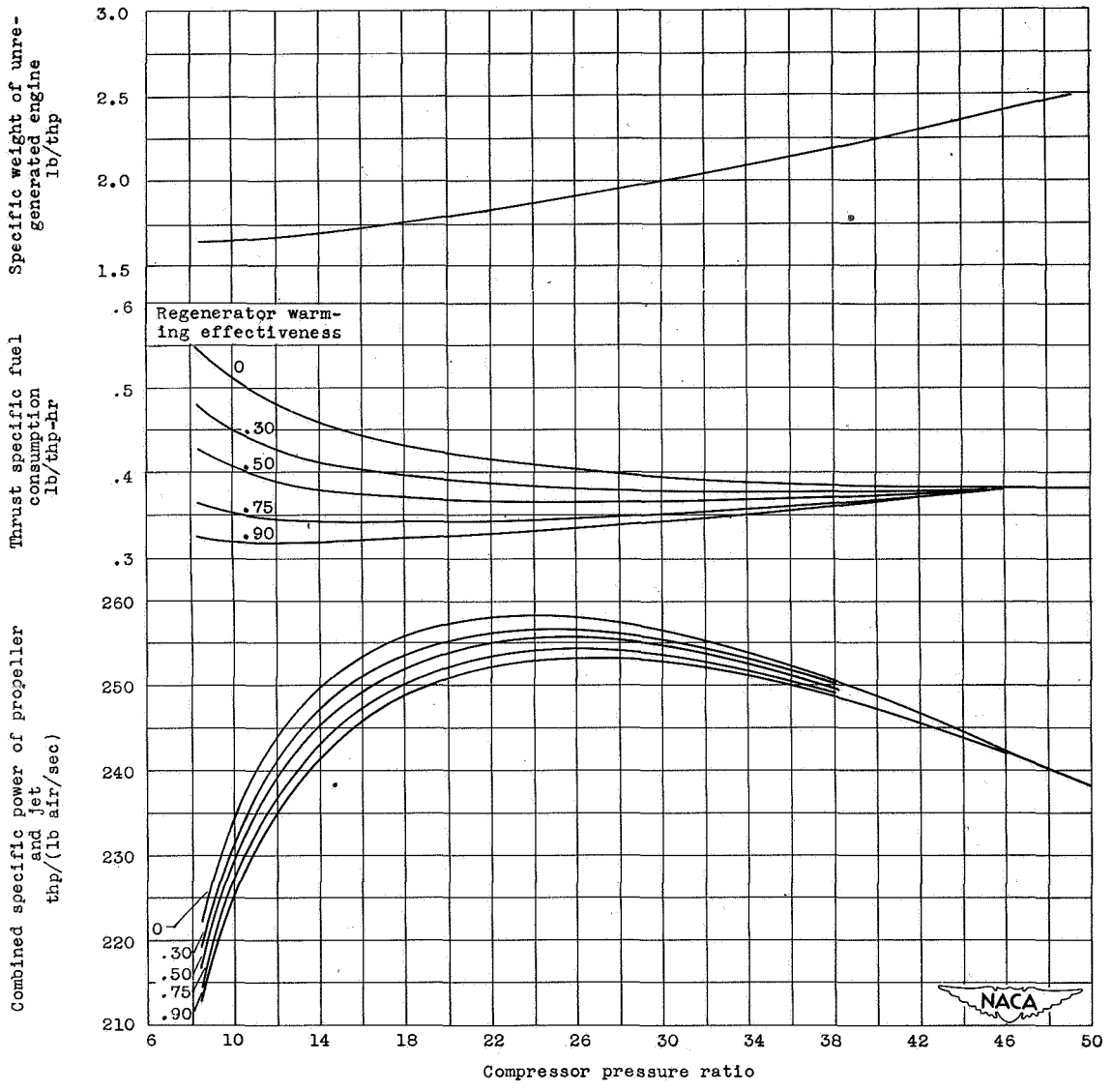

(c) Combustion temperature, 2500° F; altitude, 30,000 feet.

Figure 8. - Concluded. Specific power, thrust specific fuel consumption, and specific weight of turbine-propeller engines at various compressor pressure ratios and regenerator warming effectivenesses. Flight speed, 300 miles per hour; regenerator pressure drops, 0.

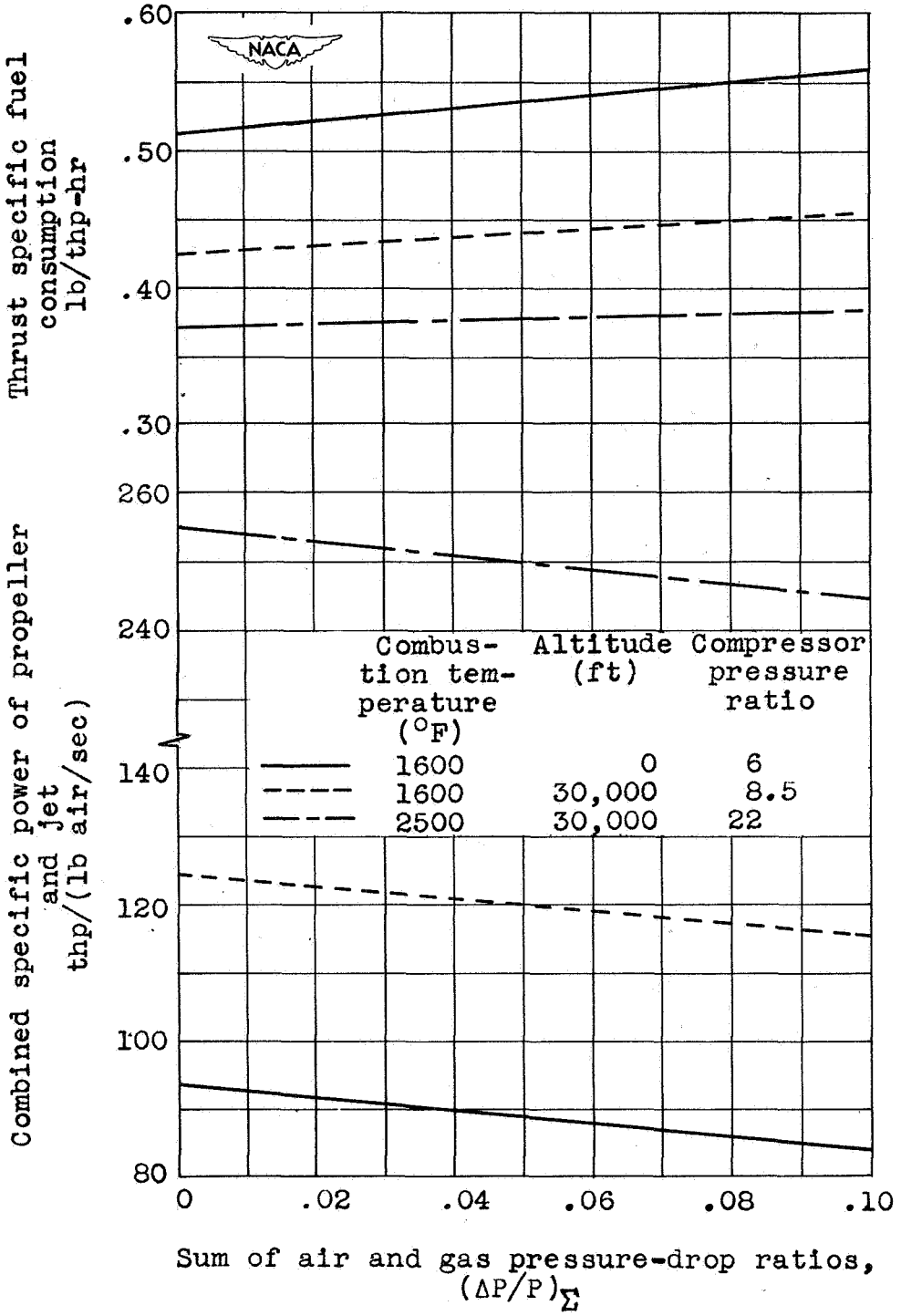

Figure 9. - Effect of regenerator pressure drops on specific power and thrust specific fuel consumption of regenerated turbine-propeller engine. Regenerator warming effectiveness, 0.5; flight speed, 300 miles per hour.

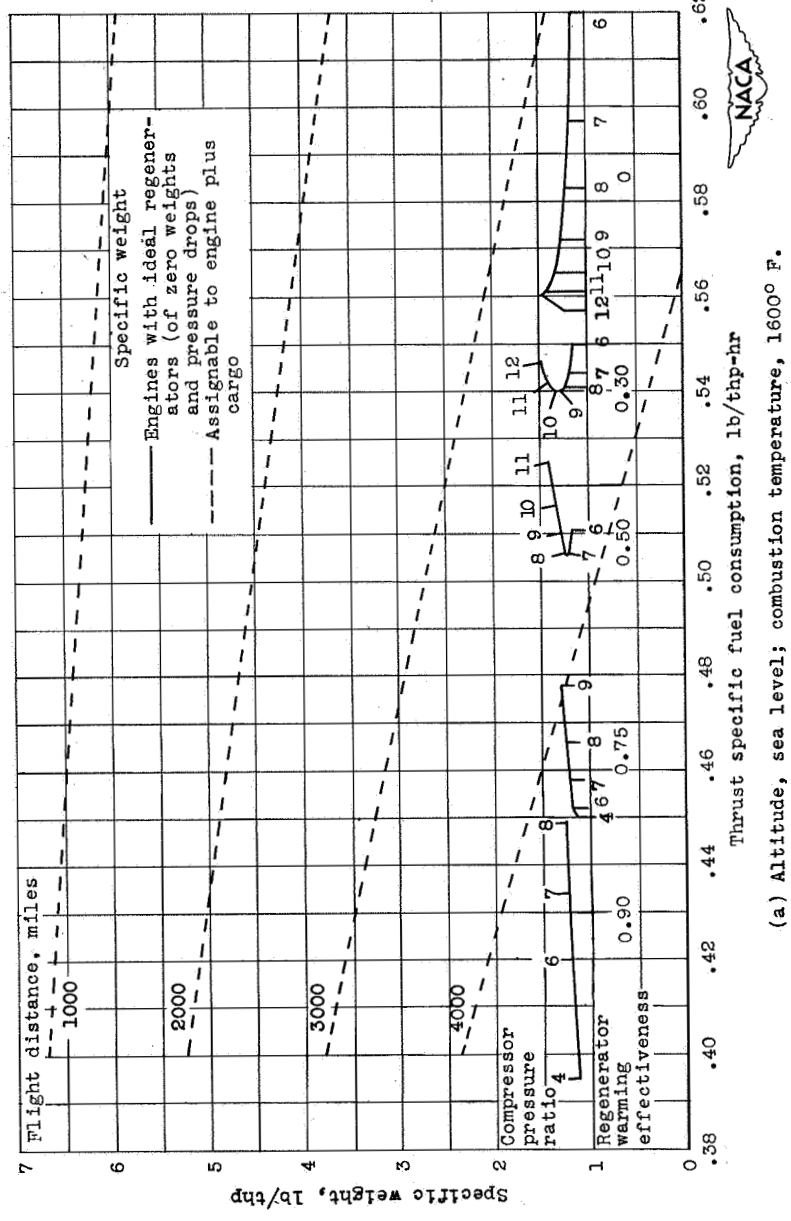

(a) Altitude, sea level; combustion temperature, 1600° F.

Figure 10. - Specific weights and thrust specific fuel consumptions of turbine-propeller engines with ideal regenerators of several regenerator warming effectivenesses on load-range coordinates. Flight speed, 300 miles per hour.

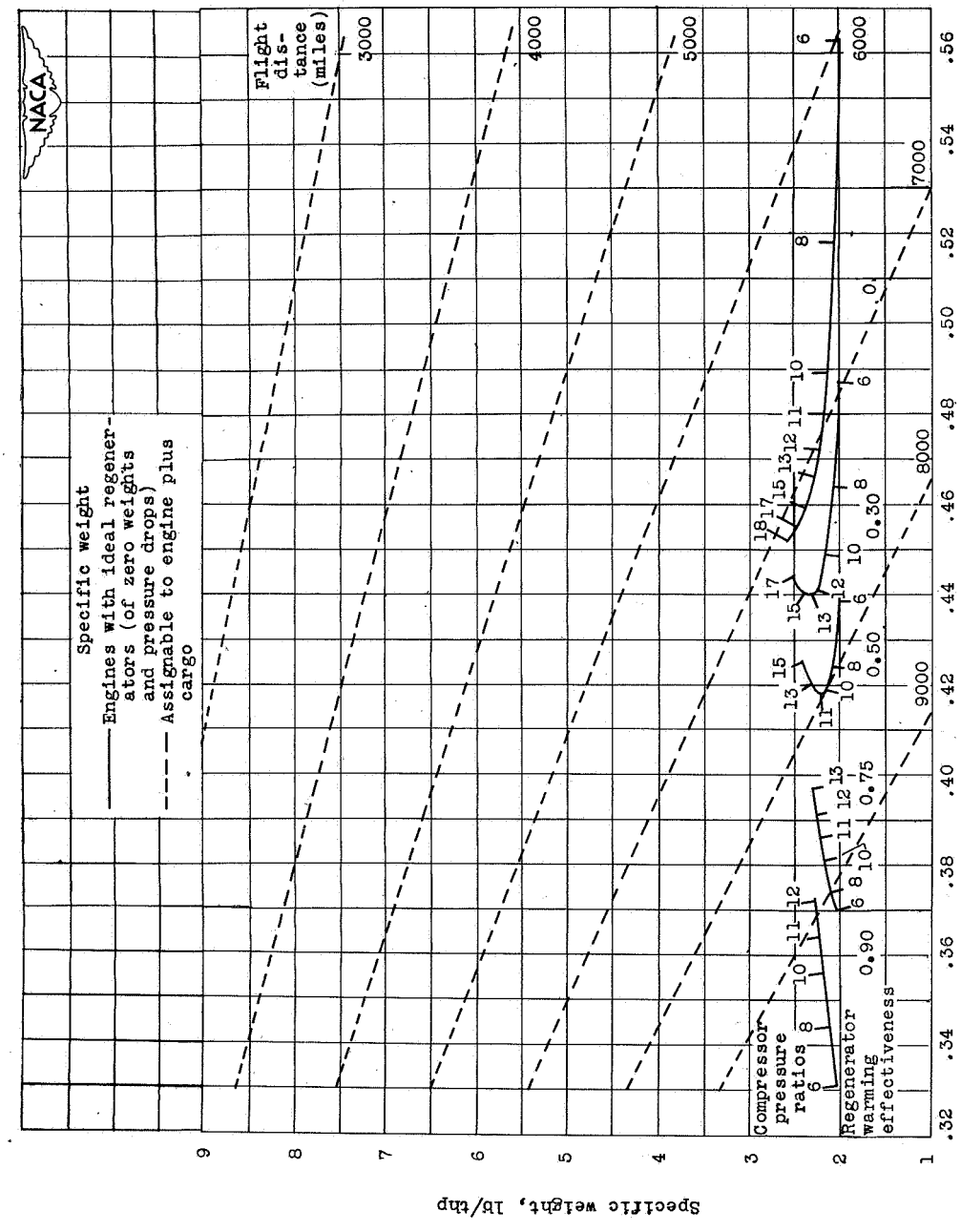

(b) Altitude, 30,000 feet; combustion temperature, 1600° F.

Figure 10. - Continued. Specific weights and thrust specific fuel consumptions of turbine-propeller engines with ideal regenerators of several regenerator warming effectivenesses on load-range coordinates. Flight speed, 300 miles per hour.

2001

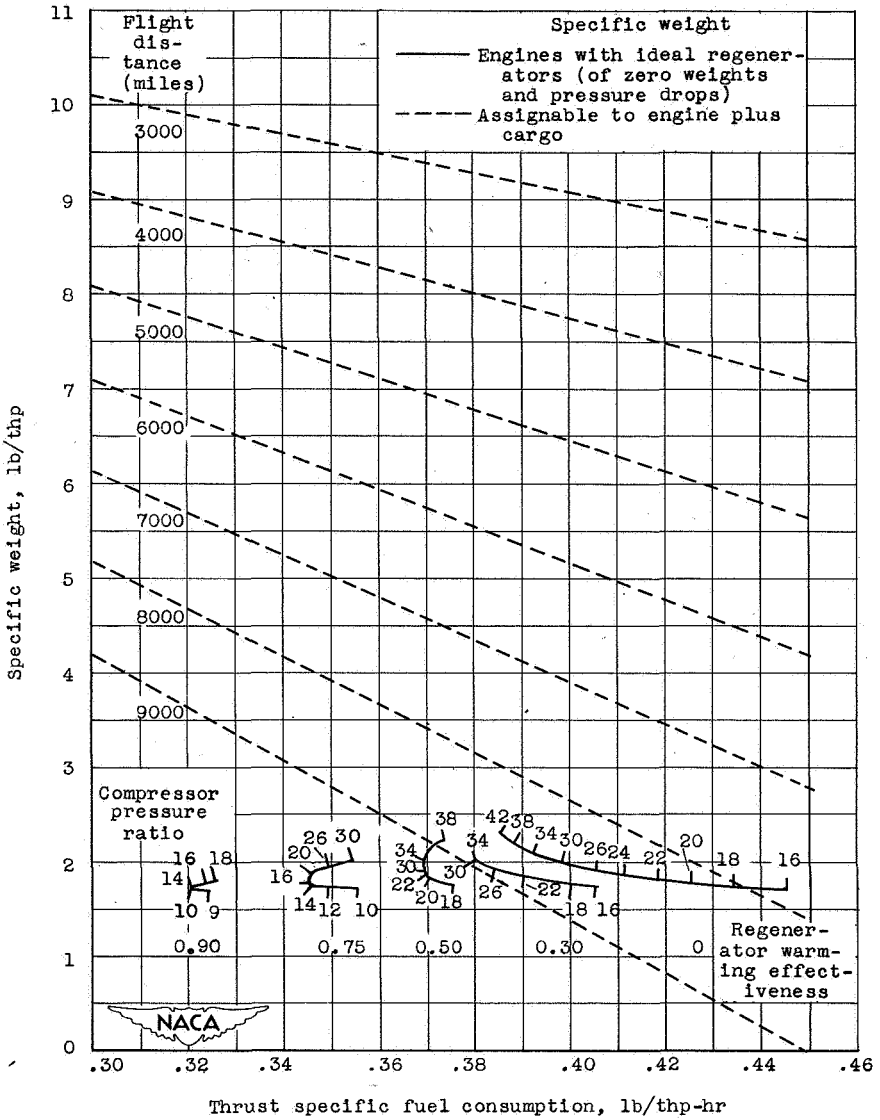

(c) Altitude, 30,000 feet; combustion temperature, 2500° F.

Figure 10. - Concluded. Specific weights and thrust specific fuel consumptions of turbine-propeller engines with ideal regenerators of several regenerator warming effectivenesses on load-range coordinates. Flight speed, 300 miles per hour.

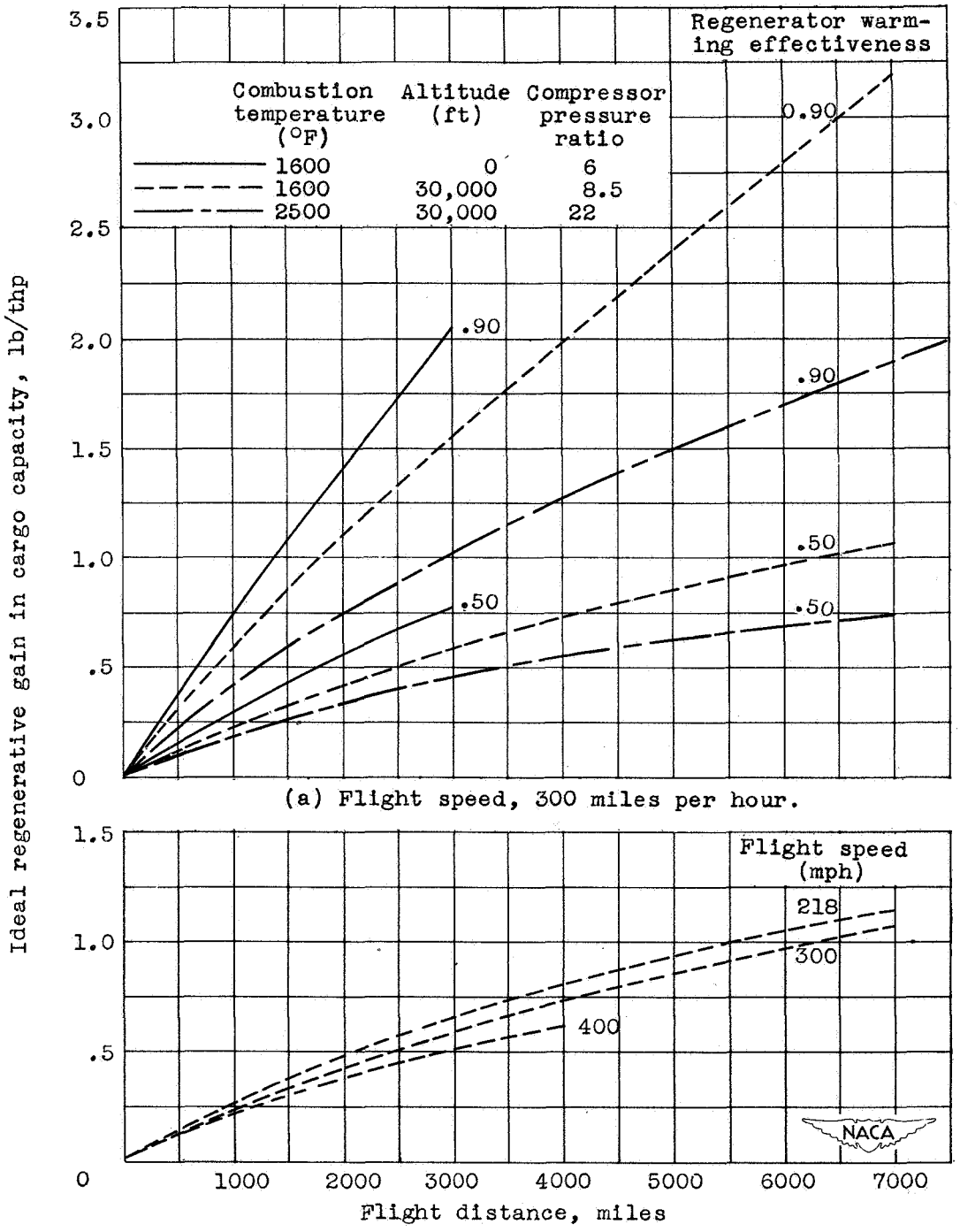

Figure 11. - Variation of gain in cargo capacity from ideal regenerators (zero weights and pressure drops) at optimum compressor pressure ratio as compared with unregenerative operation at optimum compressor pressure ratios for several altitudes, combustion temperatures, flight speeds, and regenerator warming effectivenesses.

Curve	Regenerator	Regenerator parameters, in.
aa	Crossflow plate and interrupted fin (fig. 4)	a, 0.1875; b, 0.132; t_w, 0.01; δ, 0.005; s, 0.125 to 0.50
bb	Crossflow plate and uninterrupted fin (fig. 5)	a, 1/4; (b + δ), 1/4; t_w, 0.01; δ, 0.005; s, 1/4 core O.D. 47.3 45.0 43.4 40.6 core I.D. 24.1 21.1 18.6 15.8
cc	Counterflow tubular (fig. 7)	tube I.D., 0.250; $(\Delta P/P)_\Sigma$, 0.005 to 0.05; core O.D., variable to provide range of $(\Delta P/P)_\Sigma$

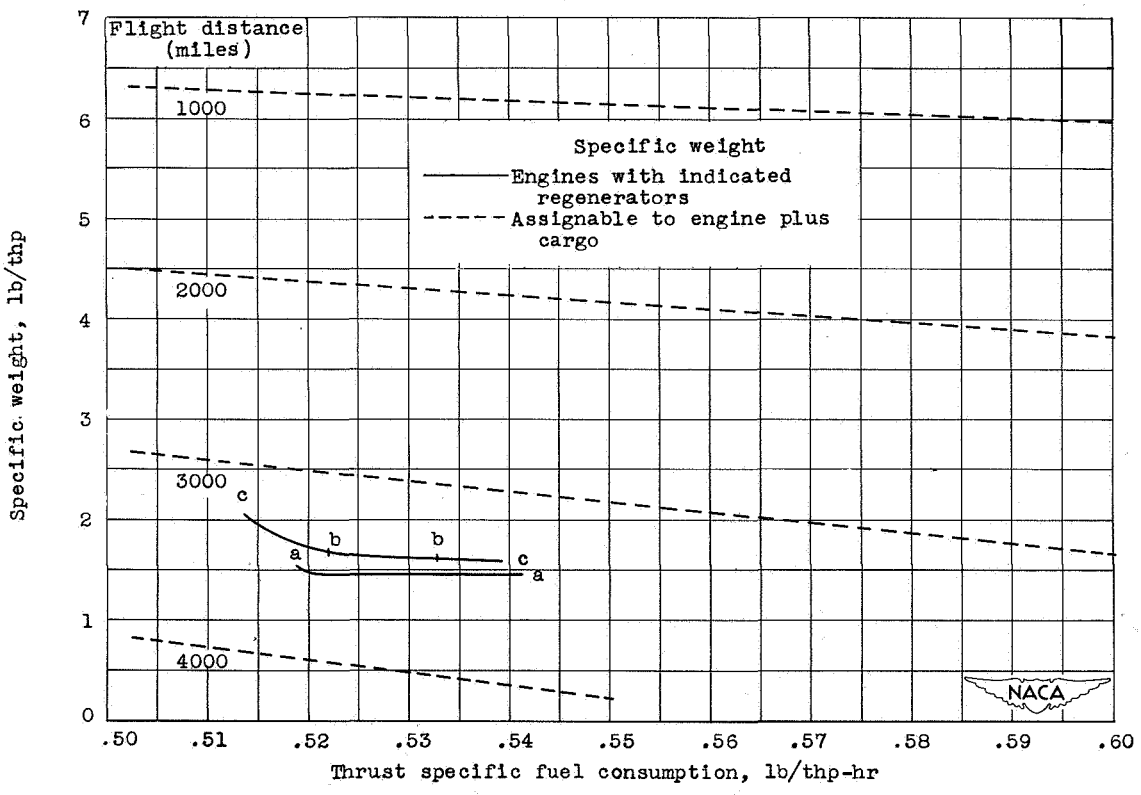

Figure 12. - Specific weights and thrust specific fuel consumptions of turbine-propeller engines with optimum series of three types of regenerator core on load-range coordinates. Altitude, sea level; combustion temperature, 1600° F; compressor pressure ratio, 6; flight speed, 300 miles per hour; regenerator warming effectiveness, 0.5.

η_R	a (in.)	b (in.)	s (in.)	t_w (in.)	δ (in.)
0.30	0.375	0.310	0.125 - 1.0	0.01	0.005
.50	.250	.252	.125 - .500		
.75	.125	.195	.075 - .500		

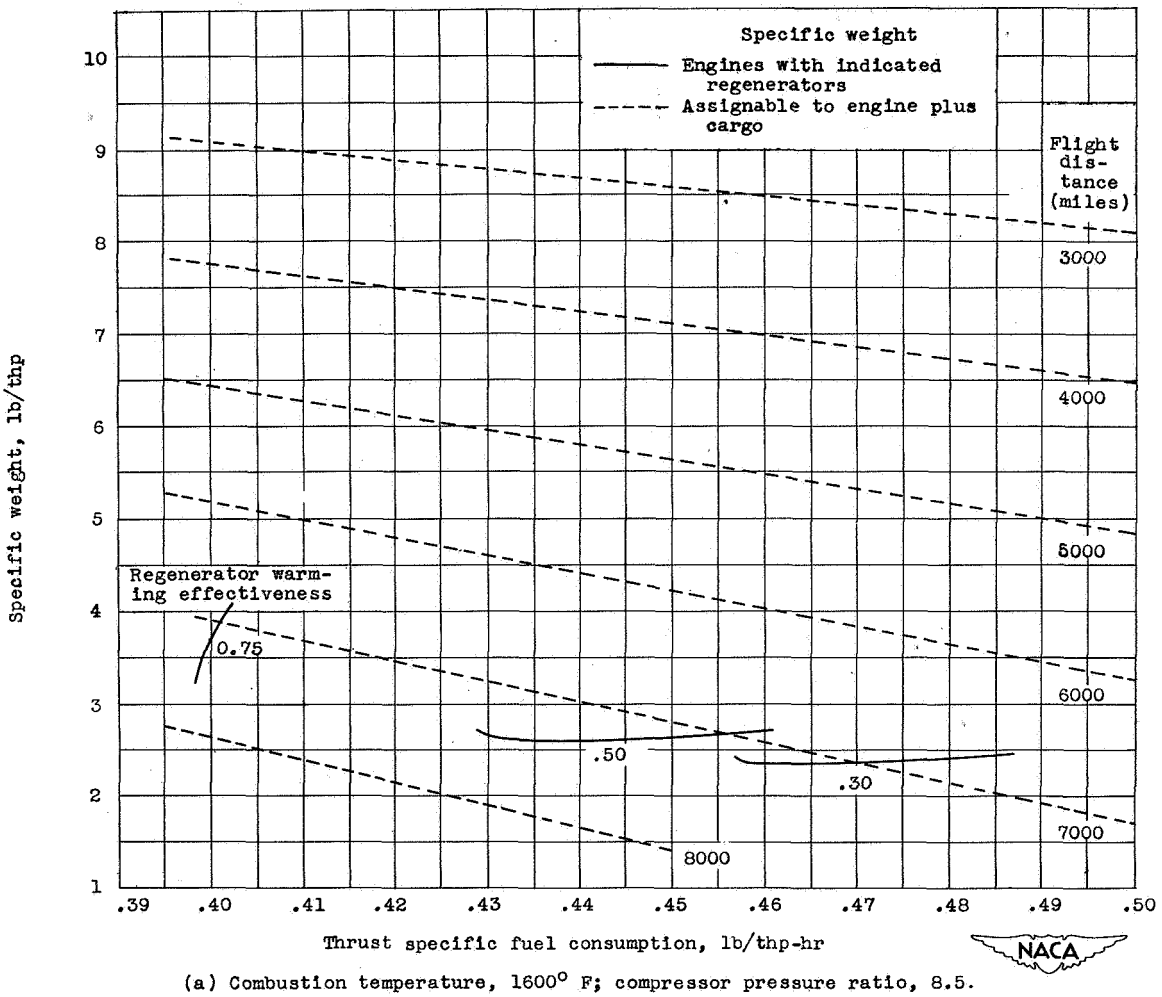

(a) Combustion temperature, 1600° F; compressor pressure ratio, 8.5.

Figure 13. - Specific weights and thrust specific fuel consumptions of turbine-propeller engines with optimum series of crossflow-plate and interrupted-fin regenerators (fig. 4) of three regenerator warming effectivenesses on load-range coordinates. Altitude, 30,000 feet; flight speed, 300 miles per hour.

η_R	a (in.)	b (in.)	s (in.)	t_w (in.)	δ (in.)
0.30	0.250	0.435	0.125 - 0.75	0.02	0.005
.50	.250	.252	.125 - .60		
.75	.125	.195	.125 - .50		

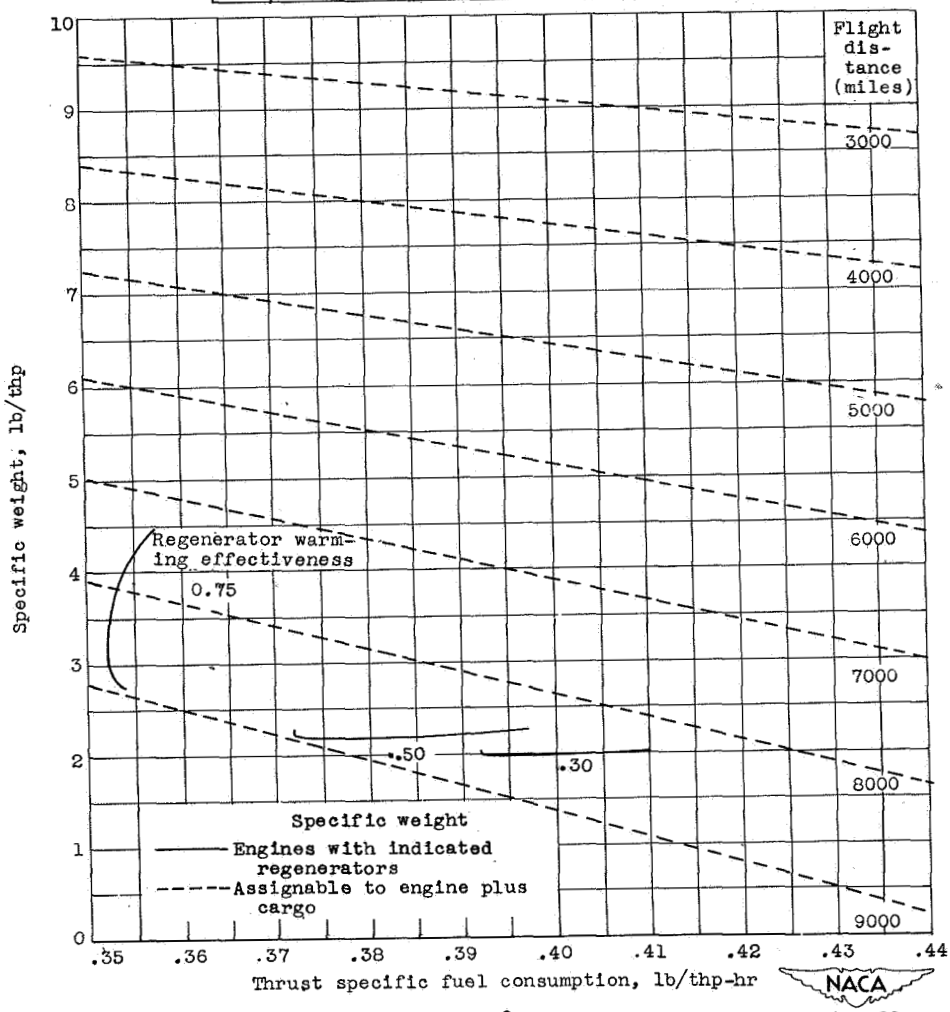

(b) Combustion temperature, 2500° F; compressor pressure ratio, 22.

Figure 13. - Concluded. Specific weights and thrust specific fuel consumptions of turbine-propeller engines with optimum series of crossflow-plate and interrupted-fin regenerators (fig. 4) of three regenerator warming effectivenesses on load-range coordinates. Altitude, 30,000 feet; flight speed, 300 miles per hour.

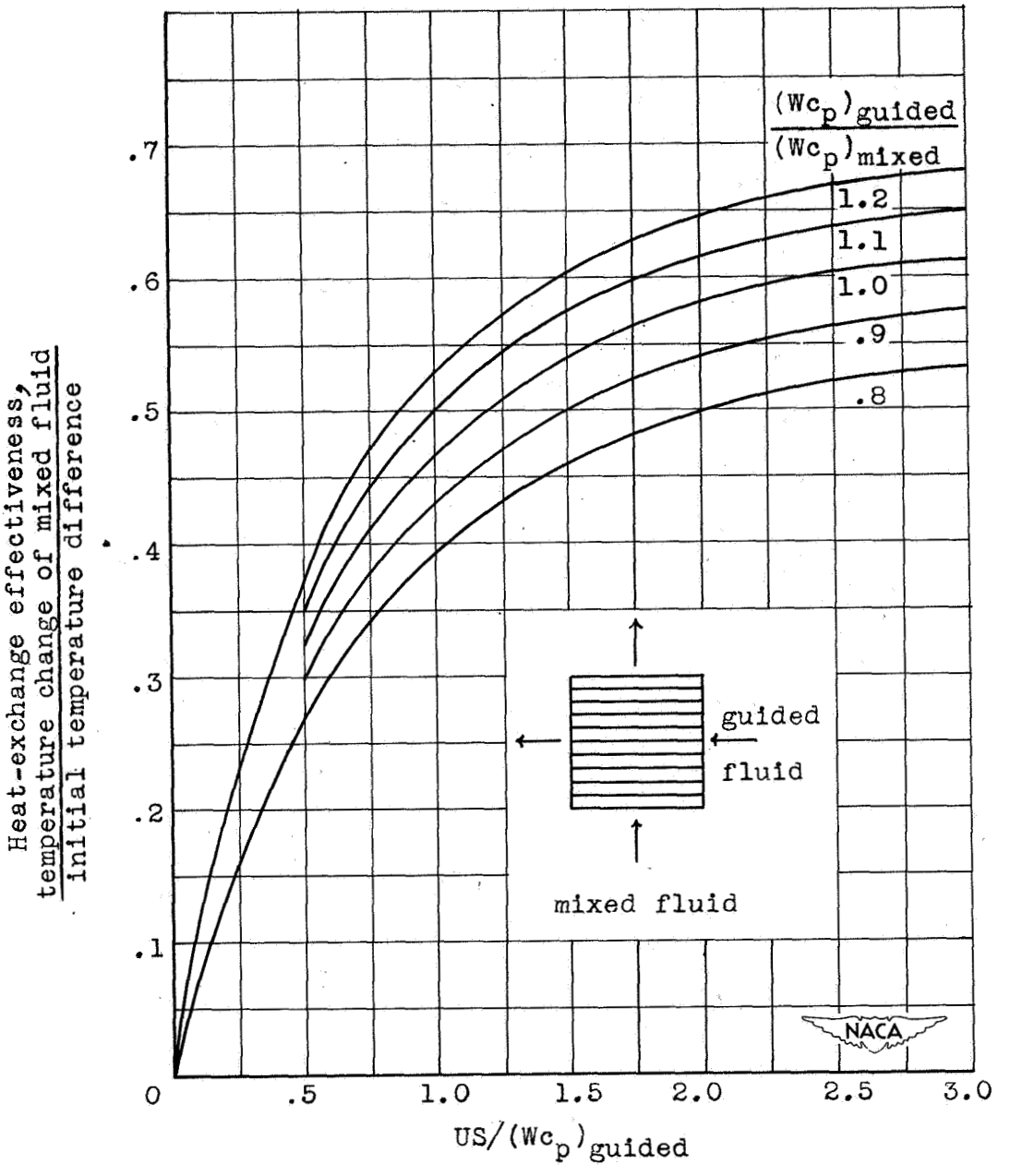

Figure 14. - Variation of heat-exchange effectiveness with $US/(Wc_p)_{guided}$ for various values of $(Wc_p)_{guided}/(Wc_p)_{mixed}$ in a single-pass crossflow heat exchanger.